Journal of Neurochemistry JNC

JOURNAL OF NEUROCHEMISTRY | 2009 | 108 | 932–944 doi: 10.1111/j.1471-4159.2008.05827.x

Effects of UCH-L1 on α-synuclein over-expression mouse model of Parkinson's disease

Toru Yasuda,* Tomoko Nihira,* Yong-Ri Ren,* Xu-Qing Cao,† Keiichiro Wada,† Rieko Setsuie,‡ Tomohiro Kabuta,‡ Keiji Wada,‡ Nobutaka Hattori,† Yoshikuni Mizuno* and Hideki Mochizuki*,†

*Research Institute for Diseases of Old Age, Juntendo University, Tokyo, Japan

†Department of Neurology, Juntendo University School of Medicine, Tokyo, Japan

‡Department of Degenerative Neurological Diseases, National Institute of Neuroscience, National Center of Neurology and Psychiatry, Tokyo, Japan

Abstract

The rare inherited form of Parkinson's disease (PD), *PARK5*, is caused by a missense mutation in *ubiquitin carboxy-terminal hydrolase-L1* (*UCH-L1*) gene, resulting in Ile93Met substitution in its gene product (UCH-L1^{Ile93Met}). *PARK5* is inherited in an autosomal-dominant mode, but whether the Ile93Met mutation gives rise to a gain-of-toxic-function or loss-of-function of UCH-L1 protein remains controversial. Here, we investigated the selective vulnerabilities of dopaminergic (DA) neurons in UCH-L1-transgenic (Tg) and spontaneous UCH-L1-null *gracile axonal dystrophy* mice to an important PD-causing insult, abnormal accumulation of α-synuclein (αSyn). Immunohistochemistry of midbrain sections of a patient with sporadic PD showed αSyn- and UCH-L1-double-positive Lewy bodies in nigral DA neurons, suggesting physical and/or functional interaction between the two proteins in human PD brain. Recombinant adeno-associated viral vector-mediated over-expression of αSyn for 4 weeks significantly enhanced the loss of nigral DA cell bodies in UCH-L1^{Ile93Met}-Tg mice, but had weak effects in age-matched UCH-L1$^{wild\text{-}type}$-Tg mice and non-Tg littermates. In contrast, the extent of αSyn-induced DA cell loss in *gracile axonal dystrophy* mice was not significantly different from wild-type littermates at 13-weeks post-injection. Our results support the hypothesis that *PARK5* is caused by a gain-of-toxic-function of UCH-L1^{Ile93Met} mutant, and suggest that regulation of UCH-L1 in nigral DA cells could be a future target for treatment of PD.

Keywords: α-synuclein, adeno-associated virus, dopaminergic neurons, Parkinson's disease, ubiquitin carboxy-terminal hydrolase-L1.

J. Neurochem. (2009) **108**, 932–944.

Parkinson's disease (PD) is a progressive neurodegenerative disorder characterized clinically by resting tremor, rigidity, akinesia, and postural instability (Farrer 2006). The major pathological hallmarks of PD are the selective loss of nigrostriatal dopaminergic (DA) neurons and the presence of intraneuronal protein inclusions termed Lewy bodies, in the surviving DA neurons. Sporadic cases represent more than 90% of total patients with PD, while there exist several inherited forms (familial PD; fPD) caused by mutations in single genes. Identification and characterization of these causative genes and their products can help us understand the molecular mechanism(s) of DA neurodegeneration in the sporadic form of PD. Seven causative genes for fPDs have been identified to date; those encoding α-synuclein (αSyn), parkin, UCH-L1, PINK1, DJ-1, LRRK2, or ATP13A2 (Farrer 2006; Ramirez *et al.* 2006).

α-Synuclein is a pre-synaptic protein potentially involved in learning, synaptic plasticity, vesicle dynamics, and dopamine synthesis (Farrer 2006). The fPD *PARK1* is caused by

Received August 26, 2008; revised manuscript received November 6, 2008; accepted November 27, 2008.

Address correspondence and reprint requests to Hideki Mochizuki, Department of Neurology, Juntendo University School of Medicine, 2-1-1 Hongo, Bunkyo-ku, Tokyo, 113-8421, Japan.
E-mail: hideki@med.juntendo.ac.jp

Abbreviations used: αSyn, α-synuclein; DA, dopaminergic; DOPAC, 2-(3,4-dihydroxyphenyl)acetic acid; fPD, familial Parkinson's disease; *gad, gracile axonal dystrophy*; hrGFP, humanized recombinant green fluorescent protein; HVA, homovanillic acid; PBS, phosphate-buffered saline; PD, Parkinson's disease; rAAV, recombinant adeno-associated virus; SN, substantia nigra; SNpc, substantia nigra pars compacta; Tg, transgenic; TH, tyrosine hydroxylase; UCH-L1, ubiquitin carboxy-terminal hydrolase-L1.

missense mutations resulting in amino acid substitutions in αSyn protein (Ala53Thr, Ala30Pro, or Glu46Lys) (Polymeropoulos *et al.* 1997; Kruger *et al.* 1998; Zarranz *et al.* 2004). Furthermore, *PARK4* is caused by duplication or triplication of *αSyn* gene (*SNCA*) locus (Singleton *et al.* 2003; Nishioka *et al.* 2006). In sporadic cases of PD, αSyn protein is the major component of Lewy bodies (Spillantini *et al.* 1997; Baba *et al.* 1998). These findings suggest an important role for αSyn protein accumulation in DA cells in the pathogenesis of PD. Previous studies also reported that over-expression of αSyn protein by using a recombinant adeno-associated viral (rAAV) or lentiviral vector caused DA neurodegeneration in rats and monkeys (Kirik *et al.* 2002, 2003; Lo Bianco *et al.* 2002; Yamada *et al.* 2004; Yasuda *et al.* 2007).

Ubiquitin carboxy-terminal hydrolase-L1 constitutes 1–2% of brain proteins and functions in the ubiquitin-proteasome system (Wilkinson *et al.* 1989; Larsen *et al.* 1996, 1998). The ubiquitin hydrolase activity of UCH-L1 is important to free reusable ubiquitin monomers. UCH-L1 protein is also known to bind to and stabilize monomeric ubiquitin molecule (Osaka *et al.* 2003). *PARK5* is caused by a missense mutation in *UCH-L1* gene resulting in Ile93Met substitution in UCH-L1 protein (UCH-L1^{Ile93Met}), and inherited in an autosomal-dominant mode (Leroy *et al.* 1998). The UCH-L1^{Ile93Met} mutant was initially shown to have decreased ubiquitin hydrolase activity (Leroy *et al.* 1998; Nishikawa *et al.* 2003). In sporadic PD cases, wild-type UCH-L1 protein is deposited in Lewy bodies (Lowe *et al.* 1990). These controversial findings initiated a debate on whether the Ile93Met mutation results in gain-of-toxic-function or loss-of-function of UCH-L1 protein. Recently, we established transgenic (Tg) mice that over-express UCH-L1^{Ile93Met} protein of human origin (Setsuie *et al.* 2007). These mice showed behavioral and pathological phenotypes of Parkinsonism at 20 weeks of age (Setsuie *et al.* 2007). On the other hand, the *gracile axonal dystrophy* (*gad*) mouse, which exhibits age-dependent sensory ataxic phenotype and motor paresis, has spontaneous intragenic deletion of mouse *Uchl1* gene and systemic lack of the UCH-L1 protein expression (Saigoh *et al.* 1999). The pathological characteristics of these mice are 'dying-back' axonal degeneration in sensory and motor nerve terminals (Oda *et al.* 1992; Miura *et al.* 1993). However, they do not seem to show any pathological changes in the nigrostriatal DA pathway, especially the loss of DA cell bodies in the substantia nigra (SN). To our knowledge, no investigator has examined the vulnerability of DA neurons in *gad* mice to PD-causing insults.

The aim of the present study was to determine the functional interaction between αSyn and UCH-L1 proteins *in vivo*. Specifically, we examined whether the DA neurotoxicity associated with accumulation of αSyn protein is influenced by UCH-L1 mutation or absence of normal UCH-L1 activities. Identification of such interaction could be useful in the design of novel gene therapies that target UCH-L1.

Materials and methods

Human brain tissue

Autopsied brain of a 69-year-old female PD patient was used in this study. The diagnosis of PD was confirmed at the Department of Neurology, Juntendo University School of Medicine. The study protocol was approved by the Human Ethics Review Committee of Juntendo University School of Medicine. The autopsied midbrain tissue was cut into blocks, immediately fixed in phosphate-buffered 4% formaldehyde for 2 days. Then the tissue blocks were immersed in phosphate-buffered saline (PBS) containing 30% sucrose until sinking. Coronal sections were cut at a thickness of 30 μm using a freezing microtome.

Mice

The Tg mice lines of UCH-L1^{Ile93Met} (line H-hI93M) and UCH-L1$^{wild\text{-}type}$ (line hWT) were generated as described previously using fertilized eggs of C57BL/6 mice (Setsuie *et al.* 2007). Male UCH-L1^{Ile93Met}-Tg mice were bred with female C57BL/6 mice (Charles River Laboratories, Kanagawa, Japan), to obtain Tg and non-Tg littermates. The latter were used in the experiment at the ages of 13 weeks (denoted as 3-month-old) and 52–57 weeks (12-month-old). Male UCH-L1$^{wild\text{-}type}$-Tg mice were bred with female C57BL/6 mice, and the obtained Tg mice were used in the experiment at the ages of 13 weeks (3-month-old) and 53–57 weeks (12-month-old). At 3 and 12 months of age, the number of DA cells in UCH-L1^{Ile93Met}-Tg mice was not significantly different from those of age-matched non-Tg littermates (Setsuie *et al.* 2007; and this study, data not shown). Male and female mice heterozygous for *gad* allele were bred, and the obtained *gad* and wild-type littermates were used in the experiments at the age of 13 weeks (3-month-old). The *gad* mice line had been backcrossed to C57BL/6 background for at least 15 generations. The experimental protocol was approved by the Ethics Review Committee for Animal Experimentation of Juntendo University School of Medicine, and all surgical operations were performed according to rules set forth by the Ethics Committee for the Use of Laboratory Animals at Juntendo University.

Preparation of rAAV vector

The plasmid pAAV-MCS (CMV promoter; Stratagene, La Jolla, CA, USA) carrying human *αSyn* cDNA (pAAV-MCS-αSyn) was constructed as reported previously (Yamada *et al.* 2004). High-titer serotype-1 rAAV (rAAV1) vector stocks were prepared as described previously (Yasuda *et al.* 2007). In brief, the plasmid pAAV-MCS-αSyn or pAAV-hrGFP (humanized recombinant green fluorescent protein; Stratagene) was co-transfected with plasmids pHelper and Pack2/1 (kindly provided by Dr. T. Shimada, Nippon Medical School, Tokyo, Japan) to HEK293 cells using a standard calcium phosphate method (Sambrook and Russell 2001). After 48 h, the cells were harvested and the crude rAAV1 vector solutions were obtained by repeated freeze/thaw cycles. After ammonium sulfate precipitation, the virus particles were dissolved in PBS and applied to OptiSeal centrifugation tube (Beckman Coulter, Inc., Fullerton,

CA, USA). After overlaying the OptiPrep solution (Axis-Shield PoC AS, Oslo, Norway), the tube was processed by GradientMaster (BioComp Instruments, Inc., New Brunswick, Canada) to prepare a gradient layer of OptiPrep. The tube was then ultracentrifuged at 20 000 *g* for 18.5 h. The fractions containing high-titer rAAV1 vectors were collected and used for the injection into mice. The number of rAAV1 genome copies was quantified by PCR within the CMV promoter region using primers 5′-GACGTCAATAATGACG-TATG-3′ and 5′-GGTAATAGCGATGACTAATACG-3′. The titer of rAAV1 vector to produce human αSyn (designated rAAV1-αSyn) was 6×10^{11} genomes/mL, and the titer of rAAV1 vector to produce hrGFP (rAAV1-hrGFP) was 6×10^{11} genomes/mL.

Stereotaxic injection of rAAV1 vectors

Mice were anesthetized with sodium pentobarbital (50 mg/kg body weight; intraperitoneally, i.p.) and positioned in a stereotaxic frame. The skull was exposed, and a small portion of the skull over the SN was removed unilaterally with a dental drill. Subsequently, rAAV1-αSyn or rAAV1-hrGFP was injected unilaterally into the SN (2 μL, 2.8 mm posterior and 1.3 mm lateral from the bregma, 4.4 mm below the dural surface, tooth bar = −2 mm) through a 5-μL Hamilton microsyringe.

The rAAV1-injected UCH-L1$^{\text{wild-type}}$-Tg, UCH-L1$^{\text{Ile93Met}}$-Tg mice, and non-Tg littermates were killed at 4-weeks post-injection, while the rAAV1-injected *gad* and wild-type littermates were killed at 4-, 8-, or 13-weeks post-injection. Mice were deeply anesthetized with sodium pentobarbital (250 mg/kg body weight; i.p.) and perfused transcardially with PBS. The brains were removed *en bloc* from the skull, and cut coronally along the anterior tangent to the median eminence. The striatal tissues were then dissected and immediately frozen on dry ice. The posterior parts of brain blocks including the entire rostrocaudal extent of the SN were fixed overnight in 4% paraformaldehyde in PBS, and immersed in PBS containing 30% sucrose until sinking. Coronal sections of the SN were cut serially at 20 μm thickness by a freezing microtome.

Antibodies and immunohistochemistry

The primary antibodies used in this study were as follows; mouse anti-human αSyn (clone LB509; diluted at 1 : 100; Zymed Laboratories Inc., South San Francisco, CA, USA), rabbit anti-UCH-L1 (1 : 1000; Ultraclone, Isle of Wight, UK), rabbit anti-hrGFP (1 : 500; Stratagene), sheep anti-tyrosine hydroxylase (TH) (1 : 5000; Calbiochem, San Diego, CA, USA), rabbit anti-dopamine transporter (DAT) (1 : 200; Chemicon International Inc., Temecula, CA, USA), and rabbit anti-active caspase-3 (1 : 500; BD Biosciences, San Jose, CA, USA) antibodies. The free-floating coronal sections of the human and mice brains were washed in a PBS medium containing 0.05% Triton X-100 (PBS-T), soaked with 10% Block Ace (Yukijirushi-Nyugyo Co., Sapporo, Japan) in PBS-T, and then incubated with the primary antibody dissolved in PBS-T containing 2% Block Ace at 4°C for 24–48 h. Subsequently, for fluorescent visualization of the antigens, the sections were incubated for 2 h in the same fresh medium containing the following secondary antibodies. For human brain sections, FITC-conjugated anti-mouse IgG and Cy3-conjugated anti-rabbit IgG antibodies (1 : 500; Jackson ImmunoResearch Laboratories, Inc., West Grove, PA, USA) were used. For mouse brain sections, FITC-conjugated anti-mouse IgG or anti-rabbit IgG antibody (1 : 500; Jackson ImmunoResearch Laboratories, Inc.) and Cy3-conjugated anti-sheep IgG antibody (1 : 500; Jackson ImmunoResearch Laboratories, Inc.) were used. Sections on the slides were mounted using Vectashield Mounting Medium with 4′,6-diamidino-2-phenylindole (DAPI) (Vector Laboratories Inc., Burlingame, CA, USA). Images were captured using a confocal laser-scanning microscope (LSM510, Zeiss, Jena, Germany). For colorimetric visualization of the antigen, the sections were incubated for 2 h in the same fresh medium containing biotinylated secondary antibody (anti-mouse, anti-rabbit, or anti-sheep IgG antibody; 1 : 500; Vector Laboratories Inc.), followed by avidin-biotin-peroxidase complex (ABC Elite; Vector Laboratories Inc.) for another 1 h. Then the sections were reacted in 0.05 M Tris-HCl buffer (pH 7.6) containing 0.04% diaminobenzidine and 0.002% hydrogen peroxide with (dark brown/purple color) or without (brown color) 0.04% nickel chloride. Images were captured using a light microscope (ACT-1, Nikon Corp., Tokyo, Japan).

Densitometric analysis of αSyn

The density of human αSyn-positive cells was quantified using the NIH Image software (National Institute of Mental Health, Bethesda, MD, USA). Every fourth 20-μm-thick serial section of the brain was immunostained for human αSyn and 10 single cells in the substantia nigra pars compacta (SNpc) randomly selected per section (4–7 sections per mice) were used for densitometric analysis (four mice per group). The two-tailed Student's *t*-test was applied to evaluate the statistical significance of the difference between groups. A p value less than 0.05 denoted the presence of statistically significant difference.

DA cell counting, measurement of striatal dopamine, 2-(3,4-dihydroxyphenyl)acetic acid (DOPAC), and homovanillic acid (HVA)

At first, every eighth 20-μm-thick serial sections of the brain were immunostained for hrGFP (for mice injected with rAAV1-hrGFP) or human αSyn (for mice injected with rAAV1-αSyn). Mice that exhibited foreign protein expression in DA cells in more than half area of the entire rostrocaudal region of the SNpc were used for the following investigations. The rostrocaudal area of the SNpc immunopositive for foreign protein was determined in each mouse and used for DA cell counting (see Table 1). In every fourth serial section, the numbers of TH- and Nissl-positive cells in the SNpc were counted both in the rAAV1-injected and intact sides, as reported previously (Mandir *et al.* 1999; Furuya *et al.* 2004). In brief, SNpc cells with nuclei optimally visible by TH immunostaining, and with nuclei, cytoplasm, and nucleoli prominently stained by Nissl staining were counted. The cell number was counted by an experimenter blinded to the genotypes of mice and rAAV1 groups. The data were expressed as percentage of the contralateral side; i.e., the cell number in the rAAV1-injected side over that in the intact side.

Frozen striatal tissues were sonicated in chilled 0.1 M perchloric acid. The samples were centrifuged (20 000 *g* for 10 min at 4°C) and the resulting supernatants were used for the measurement of dopamine, DOPAC, and HVA concentrations. The HPLC system equipped with a reverse-phase C18 column (150 × 4.6 mm; ODS-100s, Tosoh, Tokyo, Japan) and an eight-electrode coulometric electrochemical detection system (ESA-400, ESA, Inc., Chelmsford, MA, USA) was used. The concentrations of dopamine, DOPAC, and HVA were determined in nanomoles per gram of tissue weight. The data were expressed as percentage of contralateral side; that is, the

Table 1 Number of mice used in the present experiments and transduction efficiencies of rAAV1 vector

	3-month-old, 4-week post-injection		12-month-old, 4-week post-injection	
Mice, rAAV1	Number of mice[a]	Efficiency[b] (%)	Number of mice	Efficiency (%)
Wt-Tg, GFP	6/6	75.1 ± 3.4	5/5	74.7 ± 2.5
Wt-Tg, αSyn	6/7	74.3 ± 7.1	6/6	74.4 ± 4.2
I93M-Tg, GFP	4/6	68.2 ± 2.1	7/7	80.8 ± 1.5
I93M-Tg, αSyn	5/6	75.2 ± 7.9	6/7	70.4 ± 5.1
Non-Tg, αSyn	4/6	76.6 ± 5.9	5/6	68.8 ± 4.6

	3-month-old, 4-week post-injection		3-month-old, 8-week post-injection		3-month-old, 13-week post-injection	
Mice, rAAV1	Number of mice	Efficiency (%)	Number of mice	Efficiency (%)	Number of mice	Efficiency (%)
wild-type, GFP	4/4	77.6 ± 0.9	5/5	79.4 ± 5.9	5/5	76.1 ± 3.7
wild-type, αSyn	4/4	74.8 ± 1.0	5/5	73.2 ± 4.8	6/6	77.2 ± 4.6
gad, GFP	5/5	75.7 ± 0.9	5/5	77.7 ± 9.8	6/6	67.5 ± 2.1
gad, αSyn	5/5	76.1 ± 1.1	5/5	80.4 ± 6.4	7/7	77.2 ± 2.1

[a]Data are number of mice selected for DA cell count over that of total mice injected with rAAV1 vector.
[b]Transduction efficiency of rAAV1 vector was expressed as percentage of total DA cells in the SNpc; *i.e.*, the number of DA cells in the contralateral uninjected side in the area immunopositive for foreign protein relative to that in the entire rostrocaudal extent of the SNpc (mean ± SEM).
Wt-Tg, UCH-L1$^{wild\text{-}type}$-Tg; I93M-Tg, UCH-L1^{Ile93Met}-Tg.

concentration in the rAAV1-injected side over that in the intact side. One-way analysis of variance (ANOVA) followed by Tukey-Kramer's *post hoc* test was applied to evaluate the statistical differences among the groups. A p value less than 0.05 denoted the presence of statistically significant difference.

Results

Co-localization of αSyn and UCH-L1 proteins in nigral Lewy bodies in human PD brain

At first, we performed immunohistochemical analysis for αSyn and UCH-L1 proteins using a midbrain section of a patient with sporadic PD. We found several αSyn- and UCH-L1-double-positive Lewy bodies in the pigmented DA cells in the SN (Fig. 1). αSyn and UCH-L1 proteins co-localized on the halo of Lewy bodies. No fluorescent labeling was detected in the control staining lacking the primary antibodies (data not shown). These results suggested a potential physical and/or functional interaction between the two proteins in human PD brain and prompted us to examine this issue in the experimental animal model of PD.

rAAV1 vector-mediated expression of hrGFP or human αSyn protein in mouse DA neurons

The high-titer viral stocks of rAAV1-hrGFP (6×10^{11} genomes/mL) and rAAV1-αSyn (6×10^{11} genomes/mL) were prepared and injected unilaterally into the SN of 3-month-old UCH-L1$^{wild\text{-}type}$-Tg, UCH-L1^{Ile93Met}-Tg mice, and their non-Tg littermates. At 4-weeks post-injection period, mice were killed and examined for the expression of foreign proteins in the SN by immunohistochemical analysis (Fig. 2). We used a polyclonal antibody that detects hrGFP (green; Fig. 2a–d), a monoclonal antibody (clone LB509) that specifically detects αSyn protein of human origin (green; Fig. 2e–j), and anti-TH antibody that stains DA neurons (red; Fig. 2b, d, f, h, and j). The hrGFP protein was distributed uniformly in DA cell bodies (Fig. 2a and c, arrows) and neuronal processes (Fig. 2a and c, arrowheads) in the SNpc of UCH-L1$^{wild\text{-}type}$-Tg (Fig. 2a and b) and UCH-L1^{Ile93Met}-Tg mice (Fig. 2c and d). On the other hand, virally-introduced human αSyn protein was localized in the cytoplasm, processes (Fig. 2e, g, and i, arrowheads), and perinuclear region (Fig. 2e, g, and i, asterisks) of DA neurons in the SNpc of UCH-L1$^{wild\text{-}type}$-Tg (Fig. 2e and f), UCH-L1^{Ile93Met}-Tg mice (Fig. 2g and h), and non-Tg littermates (Fig. 2i and j). Immunoreactivity for human αSyn was also detected in the intranuclear space in all mice groups (co-localized with DAPI, data not shown), and no major differences were found in the distribution of αSyn protein among the groups. A similar distribution of virally-introduced αSyn was observed in the SNpc DA neurons of 12-month-old Tg and non-Tg mice (data not shown).

Importantly, densitometric analysis of human αSyn in single SNpc cells in these mice showed a significantly higher

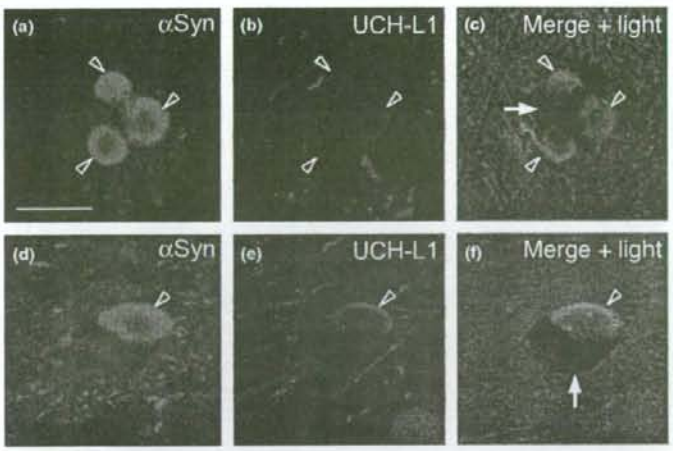

Fig. 1 Immunohistochemical analysis of αSyn and UCH-L1 proteins in the SN of human PD patient. A representative midbrain section of a patient with sporadic PD was immunostained for αSyn (green; a and d) and UCH-L1 proteins (red; b and e). Images were captured using a confocal laser-scanning microscope. Note that several Lewy bodies formed in the pigmented DA neurons (c and f; indicated by white arrows) were double-positive for αSyn and UCH-L1 proteins (a–f; open arrowheads). Scale bar in (a), 20-μm (applicable to a–f).

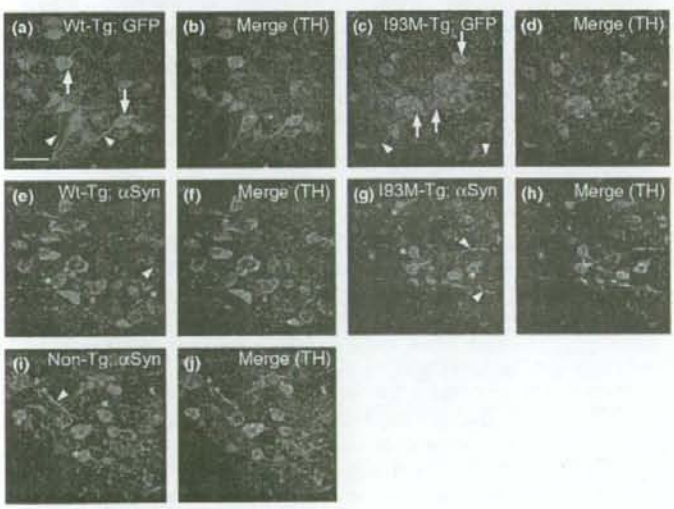

Fig. 2 Recombinant adeno-associated virus (rAAV)-mediated expression of hrGFP and human αSyn protein in mouse DA neurons in the SNpc. The distribution patterns of hrGFP (green; a–d) and αSyn protein (green; e–j) were analyzed in UCH-L1$^{wild\text{-}type}$-Tg (a, b, e, and f; denoted as Wt-Tg), UCH-L1^{Ile93Met}-Tg (c, d, g, and h; I93M-Tg), and non-Tg (i and j; Non-Tg) mice. The DA cell bodies are detected by anti-TH immunostaining (red; b, d, f, h, and j). While hrGFP protein shows a uniform distribution in DA cells and processes (a–d), αSyn is found in cytoplasm, processes (e–j, arrow heads), and perinuclear region (e–j, asterisks) of DA neurons. There are no major differences in the distribution of αSyn among all types of mice examined. Scale bar in (a), 50-μm (applicable to a–j).

immunoreactivity for αSyn in UCH-L1^{Ile93Met}-Tg mice than in UCH-L1$^{wild\text{-}type}$-Tg and non-Tg mice (Fig. 3a–d).

Next, we injected rAAV1-hrGFP or rAAV1-αSyn into the SN of 3-month-old *gad* mice and their wild-type littermates. Similarly, hrGFP protein was distributed uniformly in DA cell bodies and neuronal processes, and αSyn protein was identified in the cytoplasm, processes, perinuclear region, and intranuclear spaces of DA neurons in the SNpc of these mice with no significant difference between the groups (data not shown). As shown in Fig. 4(a)–(c), there was no significant difference in the virally-expressed αSyn between the groups at 13-weeks post-injection, as confirmed by densitometric analysis.

Effect of αSyn over-expression in UCH-L1-Tg mice

Next, we studied the effect of αSyn over-expression on the survival of DA neurons in Tg and non-Tg mice. Every fourth 20-μm-thick serial nigral section was immunostained using anti-TH antibody, followed by Nissl staining. As shown in Fig. 5, loss of DA cell bodies was observed in the SNpc of UCH-L1^{Ile93Met}-Tg mice injected with rAAV1-αSyn (compare Fig. 5e and f, and g and h; indicated by open arrowheads in e) at 4-weeks post-injection. On the other hand, injection of rAAV1-αSyn caused no apparent cell loss in UCH-L1$^{wild\text{-}type}$-Tg (Fig. 5a–d) and non-Tg mice (Fig. 5i–l) at the same time point. Immunostaining for another DA cell marker, dopamine transporter, also showed loss of DA

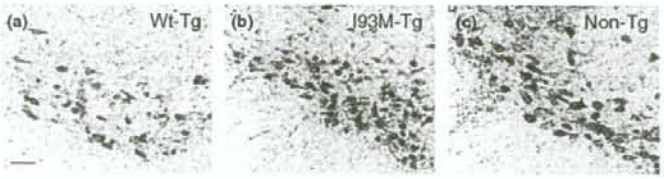

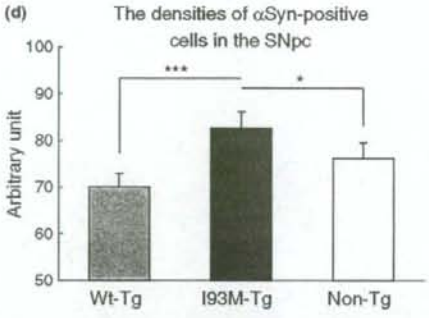

Fig. 3 Densitometric quantification of αSyn in single cells of the SNpc of UCH-L1-Tg and non-Tg mice. Nigral sections were subjected to anti-human αSyn immunostaining. Representative photographs were taken in UCH-L1$^{wild\ type}$-Tg (a; denoted as Wt-Tg), UCH-L1^{Ile93Met}-Tg (b; I93M-Tg), and non-Tg mice (c; Non-Tg). Scale bar in (a), 50-μm (applicable to a–c). (d) The density of human αSyn was quantified using 4–7 of every four serial nigral sections ($n = 4$ mice for each group). *$p < 0.05$ and ***$p < 0.001$ (two-tailed Student's *t*-test).

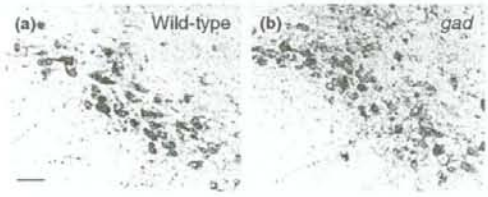

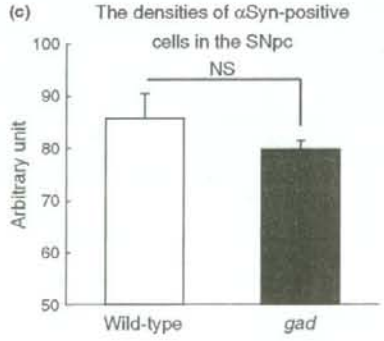

Fig. 4 Densitometric quantification of αSyn in single cells of the SNpc of wild-type and *gad* mice. Nigral sections were subjected to anti-human αSyn immunostaining. Representative photographs were taken in wild-type (a) and *gad* mice (b). Scale bar in (a), 50-μm (applicable to a and b). (c) The density of human αSyn was quantified using 4–7 of every four serial nigral sections ($n = 4$ mice for each group). n.s., not significant (two-tailed Student's *t*-test).

cell bodies in the SNpc of UCH-L1^{Ile93Met}-Tg mice injected with rAAV1-αSyn (Fig. 6a–f). Immunostaining of nigral sections of the three genetic types of mice using anti-active caspase-3 antibody showed anti-active caspase-3-immunoreactivities in the SNpc of the rAAV1-αSyn-injected side of UCH-L1^{Ile93Met}-Tg mice (Fig. 6g). These results suggest that αSyn-induced DA cell degeneration in UCH-L1^{Ile93Met}-Tg mice is mediated through apoptotic machinery. Then, we counted the number of TH- and Nissl-positive SNpc cells in both rAAV1-injected and non-injected intact sides of these mice. Immunostaining in the rostrocaudal areas of the SN for hrGFP and human αSyn varied among mice, and accordingly, we determined the immunostaining in each mouse using every eighth 20-μm-thick serial nigral section. Mice positive for the virally-introduced protein in more than half of the rostrocaudal region of the SN were selected for DA cell counting (see Materials and Methods). Table 1 provides a summary of the numbers of selected mice, rAAV1-injected mice, and transduction efficiencies of rAAV1 vector in the selected mice. In Fig. 7(a) and (b), the data are represented as % of contralateral, *i.e.*, TH- and Nissl-positive cell number in the rAAV1-injected side relative to that in the intact side. In rAAV1-αSyn-injected mice (Fig. 7a and b, solid bars), UCH-L1^{Ile93Met}-Tg mice ($n = 5$, number of animals shown in parenthesis in each bar) exhibited significant loss of DA cell bodies (~30% decrease) compared with UCH-L1$^{wild\text{-}type}$-Tg (~0% decrease) and non-Tg mice (~10% decrease). Furthermore, the relative number of DA cells in the rAAV1-αSyn-injected UCH-L1^{Ile93Met}-Tg mice was significantly lower than in rAAV1-hrGFP-injected UCH-L1^{Ile93Met}-Tg mice (Fig. 7a and b, open bars; ~0% decrease), indicating that the loss of DA cell bodies was mediated specifically by αSyn protein but not by the rAAV1 vector itself or surgical injury. In 12-month-old UCH-L1^{Ile93Met}-Tg mice, we observed a similar extent (~30% decrease) of significant degeneration of TH- and Nissl-positive DA cell bodies,

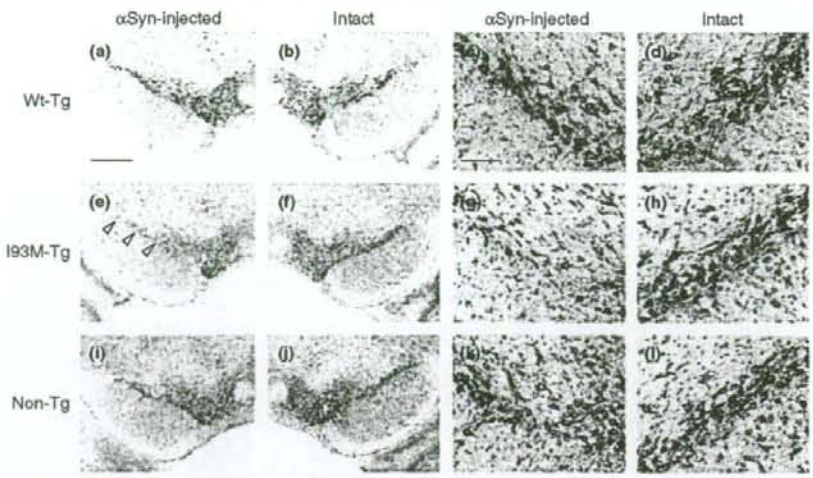

Fig. 5 α-Synuclein-induced degeneration of DA cell bodies in the SNpc of UCH-L1^{Ile93Met}-Tg mice at 4-weeks post-injection. Nigral sections were subjected to anti-TH immunostaining, followed by Nissl staining. Photographs were taken in UCH-L1$^{wild\text{-}type}$-Tg (a–d; denoted as Wt-Tg), UCH-L1^{Ile93Met}-Tg (e–h; I93M-Tg), and non-Tg mice (i–l; Non-Tg) injected with rAAV1-αSyn. The rAAV1-αSyn-injected side (a, c, e, g, i, and k; αSyn-injected) and non-injected intact side (b, d, f, h, j, and l; Intact) are shown. Panels (c), (d), (g), (h), (k), and (l) are enlarged images of (a), (b), (e), (f), (i), and (j), respectively. Note that the DA cell bodies are degenerated in UCH-L1^{Ile93Met}-Tg mice (compare e and f, and g and h; indicated by open arrowheads in e). Scale bar in (a), 500-μm (applicable to a, b, e, f, i, and j); and in (c), 100-μm (to c, d, g, h, k, and l).

which was also specifically induced by αSyn over-expression (Fig. 7a and b).

Next, we measured striatal dopamine concentrations in these mice. However, we could not detect any significant decrease in dopamine concentrations, both in 3- and 12-month-old mice, between the rAAV1-hrGFP- (Fig. 7c, open bars; % of contralateral) and rAAV1-αSyn-injected groups (solid bars) in both UCH-L1$^{wild\text{-}type}$-Tg and UCH-L1^{Ile93Met}-Tg mice, and among the three genetic types of mice in the rAAV1-αSyn-injected groups. There were also no significant changes in the concentrations of dopamine metabolites; DOPAC and HVA (data not shown).

Effects of αSyn over-expression in *gad* mice

Finally, we investigated the effect of viral introduction of αSyn in *gad* and their wild-type littermates. The rAAV1-injected mice were selected for the following investigations based on the criteria described above (see also Table 1). At 13-weeks post-injection period, anti-TH- and Nissl-double-staining of nigral sections manifested an rAAV1-αSyn-induced decrease of DA cell bodies in the SNpc of *gad* (Fig. 8e–h) and wild-type mice (Fig. 8a–d). When the number of the SNpc DA cell bodies was counted, we found that the rAAV1-αSyn-induced DA cell loss was significant both in *gad* and wild-type mice at 13-weeks post-injection period (Fig. 9a and b). We also found that there were no significant differences between the rAAV1-αSyn-injected *gad* and wild-type groups at 4- (~10% decrease, Fig. 9a and b), 8- (~20% decrease), and 13-weeks post-injection (~25% decrease), while the rAAV1-αSyn-induced DA cell loss was not yet significant in *gad* mice compared with the rAAV1-hrGFP-injected group at 8-weeks post-injection.

There was no significant decrease in striatal dopamine concentrations at both 8- and 13-weeks post-injection, between the rAAV1-hrGFP- (Fig. 9c, open bars; % of contralateral) and rAAV1-αSyn-injected groups (solid bars), in both wild-type and *gad* mice, and between wild-type and *gad* mice in the rAAV1-αSyn-injected groups. Furthermore, the level of dopamine metabolites, DOPAC and HVA, were not changed in all groups (data not shown).

Discussion

In the present study, based on the previous findings that αSyn and UCH-L1 proteins interact physically in a cell model of PD (Zhou *et al.* 2004) and normal mammalian brain (Liu *et al.* 2002), and are deposited in Lewy bodies in sporadic cases of PD (Lowe *et al.* 1990; Spillantini *et al.* 1997; Baba *et al.* 1998), we performed a fluorescent double-immunolabeling analysis for the two proteins using a midbrain section of a patient with sporadic PD. Co-localization of αSyn and UCH-L1 proteins in the halo of several Lewy bodies (Fig. 1) encouraged us to examine the potential functional interaction between the two proteins in a mouse model of PD; in

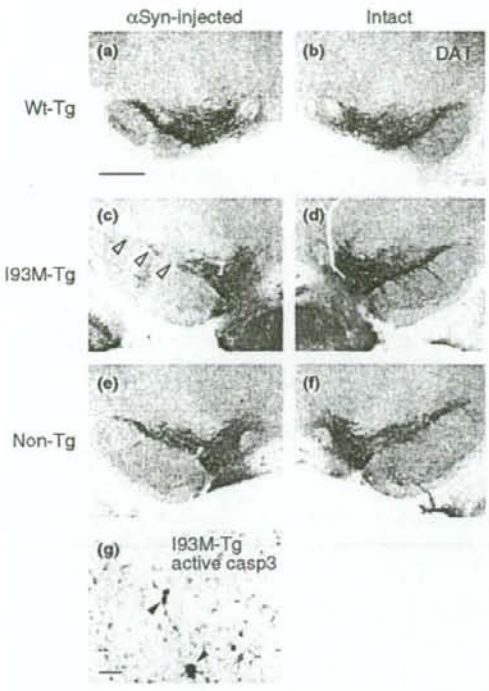

Fig. 6 α-Synuclein-induced degeneration of DA cell bodies examined by anti-DAT- and anti-active caspase-3-immunostaining. Photographs of anti-DAT immunostaining were taken in UCH-L1$^{wild\text{-}type}$-Tg (a, b; denoted as Wt-Tg), UCH-L1^{Ile93Met}-Tg (c, d; I93M-Tg), and non-Tg mice (e, f; Non-Tg) injected with rAAV1-αSyn. The rAAV1-αSyn-injected side (a, c, and e; αSyn-injected) and non-injected intact side (b, d, and f; Intact) are shown. Note the degenerated DA cell bodies in UCH-L1^{Ile93Met}-Tg mice (compare c and d; open arrowheads in c). Immunoreactivity for active caspase-3 (active casp3) is present in the SNpc of UCH-L1^{Ile93Met}-Tg mice injected with rAAV1-αSyn (g; solid arrowheads). Sections were subjected to Nissl counter-staining. Scale bar in (a), 500-μm (applicable to a–f); and in (g) 25-μm.

particular, whether UCH-L1 affects DA neurotoxicity of abnormally accumulated αSyn protein. The αSyn immunoreactivity on the halo of Lewy bodies was consistent with a previous report, which showed localization of αSyn at peripheral portions of Lewy bodies by immunoelectron microscopic analysis (Baba *et al.* 1998). We investigated αSyn-induced DA neurodegeneration in UCH-L1-Tg and -null mice by using the rAAV-mediated gene delivery. In the 4-week-period of rAAV1-mediated αSyn over-expression (shown in Figs 2 and 3), immunoreactivities for human αSyn in single SNpc cells increased significantly in UCH-L1^{Ile93Met}-Tg mice compared with UCH-L1$^{wild\text{-}type}$-Tg and non-Tg mice (Fig. 3). In this regard, we recently reported that the UCH-L1^{Ile93Met} protein inhibits chaperone-mediated autophagy through abnormally enhanced interaction between the UCH-L1 mutant and LAMP-2A protein (Kabuta and Wada 2008; Kabuta *et al.* 2008a). Such abnormal function of UCH-L1^{Ile93Met} protein might have influenced the accumulation of αSyn in the present model. Furthermore, the loss of DA cell bodies was significantly enhanced in the SNpc of UCH-L1^{Ile93Met}-Tg mice, while it was not yet apparent in UCH-L1$^{wild\text{-}type}$-Tg and non-Tg mice at 4-weeks post-injection (Figs 5–7). We also found that αSyn-induced DA neurodegeneration in UCH-L1^{Ile93Met}-Tg mice occurred through an apoptotic mechanism (Fig. 6). In a pilot experiment, we found a significant decrease in the number of nigral DA cell bodies at 8- and 13-weeks post-injection of rAAV1-αSyn, but the number was not significantly different from that of UCH-L1$^{wild\text{-}type}$-Tg, UCH-L1^{Ile93Met}-Tg, and non-Tg mice. Thus, the present results indicate that the DA neurotoxicity of αSyn protein is markedly enhanced in the presence of UCH-L1^{Ile93Met} protein. Furthermore, we found that αSyn over-expression at 13 weeks (Fig. 4) was associated with a significant DA neurodegeneration in *gad* mice, although the extent of DA cell loss was not significantly different than their wild-type littermates (Figs 8 and 9). These results indicate that the αSyn protein-induced DA neurotoxicity is not altered in the absence of UCH-L1$^{wild\text{-}type}$ protein. The striatal levels of dopamine and its metabolites, DOPAC and HVA, did not change during the period of our study (Figs 7c and 9c). In a recent study, Gorbatyuk *et al.* (2008) reported that serotype-5 rAAV-mediated over-expression of human wild-type αSyn caused a significant decrease in the number of TH- and Nissl-positive cells in the SNpc of rats at 8-weeks post-injection, while the striatal level of dopamine showed no significant decrease. Such discrepancy in the rodent models may because of the difficulty of rAAV particles to fully infiltrate the entire rostrocaudal part of the SN (Table 1), as we have suggested in a previous study (Yamada *et al.* 2004). Alternatively, the relatively slow progression of DA neurodegeneration in this model, compared with other drug-induced PD animal models, might have enabled a feedback overproduction of dopamine in the surviving and/or uninfected DA neurons.

Initially, it was reported that the *PARK5*-associated UCH-L1^{Ile93Met} mutant results in ~50% decrease in its ubiquitin hydrolase activity (Leroy *et al.* 1998; Nishikawa *et al.* 2003). Considered with the fact that *PARK5* has so far been identified in only one German kindred, without absolute penetration (Leroy *et al.* 1998), it is debatable whether *PARK5* is caused by a dominant gain-of-toxic-function or haploinsufficiency, *i.e.*, loss-of-function. In this regard, our recent study showed an age-dependent nigrostriatal DA neurodegeneration in a Tg mice line over-expressing human UCH-L1^{Ile93Met} protein (Setsuie *et al.* 2007). Although the level of transgene expression in the UCH-L1^{Ile93Met}-Tg mice line decreased gradually with aging (Setsuie *et al.* 2007) and the number of nigral DA cell bodies in aged UCH-L1^{Ile93Met}-

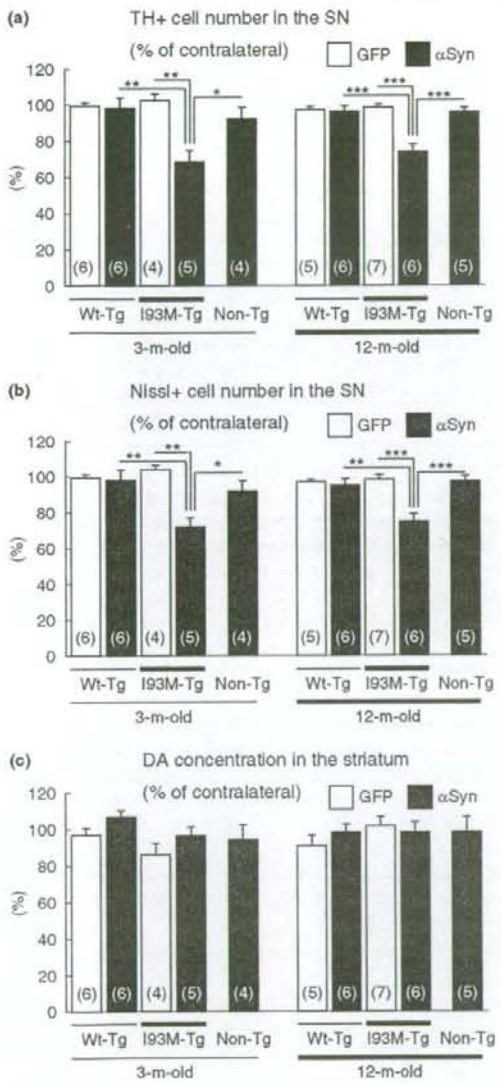

Fig. 7 Dopaminergic cell numbers in the SNpc and dopamine levels in the striatum of UCH-L1-Tg and non-Tg mice at 4-weeks post-injection. The TH- (a) and Nissl-positive cells (b) in the SNpc were counted in 3- and 12-month-old UCH-L1$^{\text{wild-type}}$-Tg (Wt-Tg), UCH-L1$^{\text{Ile93Met}}$-Tg (I93M-Tg), and non-Tg mice (Non-Tg). Data are % of those in the contralateral side. *Open bars:* rAAV1-hrGFP-injected groups, *solid bars:* rAAV1-αSyn-injected groups. The number of analyzed mice in each group is indicated within the bars. Data are mean ± SEM. $^{*}p < 0.05$, $^{**}p < 0.01$, and $^{***}p < 0.001$ (one-way ANOVA followed by Tukey-Kramer's *post hoc* test). Note that the numbers of DA cells are significantly lower in rAAV1-αSyn-injected UCH-L1$^{\text{Ile93Met}}$-Tg mice than in UCH-L1$^{\text{wild-type}}$-Tg and non-Tg mice both in 3- and 12-month-old mice. Significant differences were also found between the rAAV1-hrGFP- and rAAV1-αSyn-injected groups in UCH-L1$^{\text{Ile93Met}}$-Tg mice both at 3- and 12-months of age. (c) The striatal levels of dopamine measured in rAAV1-injected mice. Data are % of those in the contralateral side. *Open bars:* rAAV1-hrGFP-injected groups, *solid bars:* rAAV1-αSyn-injected groups. The number of analyzed mice in each group is indicated within the bars. Data are mean ± SEM. There were no significant differences in dopamine levels among the examined groups.

Tg mice was not significantly different from age-matched non-Tg littermates (data not shown), our present investigation demonstrated that the rAAV1-αSyn-induced DA cell loss was not influenced by the age of UCH-L1$^{\text{Ile93Met}}$-Tg mice. These results also suggest that the DA neurotoxicity of UCH-L1$^{\text{Ile93Met}}$ protein alone might be relatively weak in the absence of abnormal accumulation of αSyn. In this regard, a recent study showed no significant change in endogenous αSyn in UCH-L1$^{\text{Ile93Met}}$-Tg mice (Setsuie *et al.* 2007). Based on the finding that the normal aging process is associated with a significant accumulation of αSyn protein in the SN of human brain (Li *et al.* 2004; Chu and Kordower 2007), we speculate that the toxicity of accumulated αSyn might be enhanced by the UCH-L1$^{\text{Ile93Met}}$ protein in *PARK5* carriers, leading to a critical loss of DA cells and subsequent development of PD symptoms. The precise mechanism for mutated UCH-L1-mediated toxicity in the presence of accumulated αSyn should be clarified in future studies.

Several studies have reported that the over-expressed αSyn functions as a protective molecule in neuronal cells other than DA neurons (da Costa *et al.* 2000; Xu *et al.* 2002; Chandra *et al.* 2005). The selective vulnerability of DA cells in PD could be explained by the findings that αSyn protein could be covalently bound to dopamine (Conway *et al.* 2001) or could be conformationally changed by interaction with dopaminochrome *in vitro* (Norris *et al.* 2005). Both these mechanisms could lead to altered aggregation propensity, exerting a selective toxicity against culture DA cells (Xu *et al.* 2002), and elevation of intracellular catecholamine level (Mosharov *et al.* 2006). UCH-L1 is also reported to undergo oxidative modification in the brains of patients with PD and Alzheimer's disease (Choi *et al.* 2004). Furthermore, we reported recently that carbonyl-modified UCH-L1 shares aberrant molecular properties with UCH-L1$^{\text{Ile93Met}}$, including similar secondary structural changes, increased insolubility, and elevated interaction with various proteins such as tubulin (Kabuta *et al.* 2008b). We speculate that such post-translational modification, or perhaps another yet unidentified modification(s), could potentially induce the neurotoxic activity of UCH-L1, rendering the accumulated αSyn protein neurotoxic to nigral DA neurons in patients with the sporadic form of PD.

On the other hand, our present study showed that nigral DA cells were killed to no more/lesser extent by the

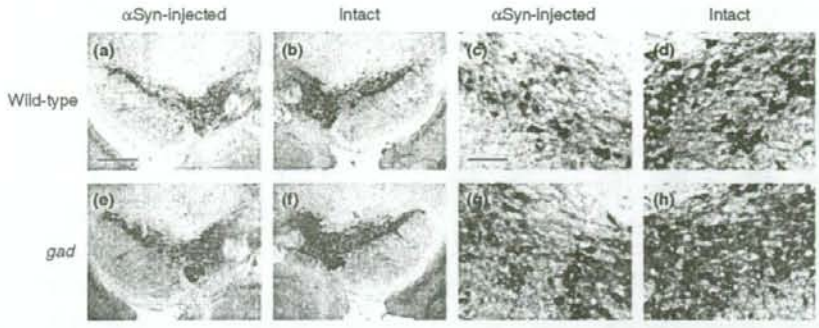

Fig. 8 α-Synuclein-induced degeneration of DA cell bodies in the SNpc of wild-type and *gad* mice at 13-weeks post-injection. Nigral sections were subjected to anti-TH immunostaining, followed by Nissl staining. Photographs were taken in wild-type littermate (a–d) and *gad* mice (e–h) injected with rAAV1-αSyn. The rAAV1-αSyn-injected side (a, c, e, and g; αSyn-injected) and non-injected intact side (b, d, f, and h; Intact) are shown. Panels (c), (d), (g), and (h) are enlarged images of (a), (b), (e), and (f), respectively. Note the degeneration of DA cell bodies in the rAAV1-αSyn-injected sides in both the wild-type and *gad* mice. Scale bar in (a), 500-μm (applicable to a, b, e, and f); and in (c), 100-μm (to c, d, g, and h).

injection of rAAV1-αSyn in the absence of UCH-L1 protein, *i.e.*, in *gad* mice. Previous pathological studies in *gad* mice suggested that UCH-L1 has important roles in the survival of certain neuronal populations, such as sensory and motor neurons (Oda *et al.* 1992; Miura *et al.* 1993). Recent reports also showed that UCH-L1 protein is involved in the survival of other types of neuronal cells. In birds and mice, up-regulation of UCH-L1 is associated with increased survival of replaceable neurons, which continue to be produced and replaced in adulthood (Lombardino *et al.* 2005). Moreover, transduction of exogenous UCH-L1 protein protected against β-amyloid-induced synaptic dysfunction of hippocampal neurons *in vitro* and improved the retention of contextual learning in a mouse model of Alzheimer's disease (Gong *et al.* 2006). As mentioned above, UCH-L1 protein is oxidatively modified and down-regulated in the frontal cortex of patients with sporadic PD and Alzheimer's disease (Choi *et al.* 2004). We reported that oxidation of UCH-L1 protein by 4-hydroxynonenal resulted in a loss of ubiquitin hydrolase activity *in vitro* (Nishikawa *et al.* 2003). In another study, we also reported that UCH-L1 bound to and stabilized monomeric ubiquitin molecule *in vivo*; the level of monomeric ubiquitin was significantly decreased in various brain structures of *gad* mice (Osaka *et al.* 2003). Moreover, proteomic analysis of proteins isolated from the cortical area of *gad* brain revealed oxidative modification of several key proteins possibly linked to neurodegeneration (Castegna *et al.* 2004). However, it is still unknown whether such modification of proteins does occur in the nigral DA cells of *gad* mice. Indeed, no pathological changes have been reported in the SN of *gad* mice. When we counted the number of TH- and Nissl-double-positive DA cells in the entire rostrocaudal extent of the SNpc of *gad* mice, there was no significant difference with wild-type mice (data not shown). Thus, we add an alternative scenario; functional loss of UCH-L1 might have neuroprotective effects. The present study showed that there was no significant decrease in DA cells in *gad* mice between rAAV1-hrGFP-injected and rAAV1-αSyn-injected groups at 8-weeks post-injection, while there was a significant one in wild-type mice (Fig. 9a and b). These results could imply the potential deleterious effects of normal UCH-L1, which were suggested previously by Liu *et al.* (2002). Recently, we reported that retinal neurons in *gad* mice were resistant to ischemic injury (Harada *et al.* 2004). Ischemic stress induces UCH-L1-mediated up-regulation of ubiquitin in wild-type mice, but high levels of ubiquitin induced caspase-dependent retinal neuronal apoptosis (Harada *et al.* 2004). We speculate that another closely related ubiquitin hydrolyzing enzyme, UCH-L3, might have complemented the loss of UCH-L1. The UCH-L1- and UCH-L3-double-null mice show more severe neurodegenerative phenotypes than *gad* mice (Kurihara *et al.* 2001); accordingly, the vulnerability of their nigrostriatal DA neurons to αSyn accumulation should be analyzed in detail in the future. However, the present results demonstrated clearly that the loss of UCH-L1 protein does not cause any harmful or protective effect on prolonged abnormal accumulation of αSyn in nigral DA cells.

In conclusion, our study showed that accumulated αSyn protein is neurotoxic to DA neurons and that such neurotoxicity is enhanced by *PARK5*-associated UCH-L1^{Ile93Met} mutant, but not influenced by the loss of UCH-L1$^{wild\text{-}type}$ protein *in vivo*. Accordingly, we believe that the present results support the hypothesis of dominant gain-of-toxic-function mutation of UCH-L1 as the cause of *PARK5*. Considering the possibility that the UCH-L1$^{wild\text{-}type}$ protein might be toxic by certain age-dependent post-translational

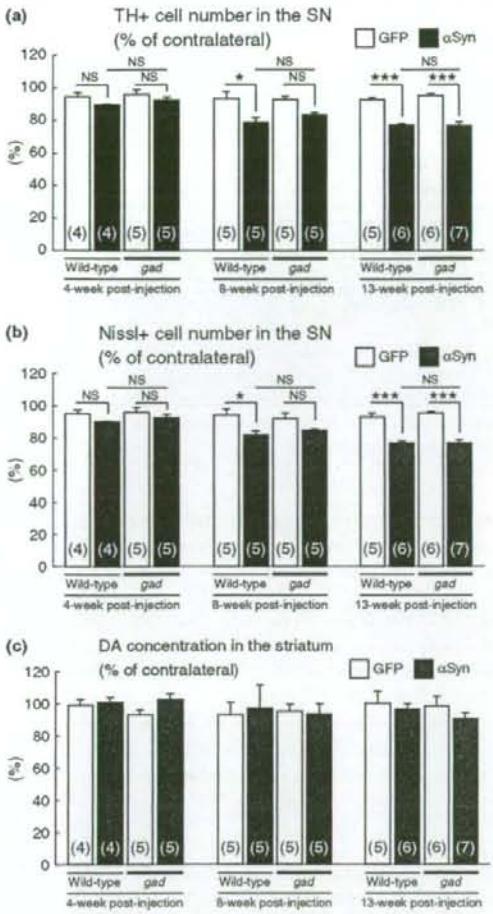

Fig. 9 Dopaminergic cell number in the SNpc and dopamine concentration in the striatum of wild-type and *gad* mice at 4-, 8-, and 13-weeks post-injection. The TH- (a) and Nissl-positive cells (b) in the SNpc were counted in 3-month-old mice. Data are % of the numbers in the contralateral side. *Open bars:* rAAV1-hrGFP-injected groups, *solid bars:* rAAV1-αSyn-injected groups. The number of analyzed mice in each group is indicated within the bars. Data are mean ± SEM. $^{*}p < 0.05$, $^{***}p < 0.001$, and n.s., not significant (one-way ANOVA followed by Tukey-Kramer's *post hoc* test). Note the lack of significant differences between the rAAV1-αSyn-injected wild-type and *gad* groups both at 8- and 13-weeks post-injection. (c) The striatal levels of dopamine were measured in the rAAV1-injected mice. Data are % of the levels in the contralateral side. *Open bars:* rAAV1-hrGFP-injected groups, *solid bars:* rAAV1-αSyn-injected groups. The number of analyzed mice in each group is indicated within the bars. Data are mean ± SEM. There were no significant differences in dopamine levels in the examined groups.

modifications in DA neurons, elucidation of the entire functions of fPD-linked causative gene products and functional interactions among them should provide new insights into the molecular pathogenesis and clinical approaches for the sporadic form of PD.

Acknowledgements

This work was supported by a High Technology Research Center grant, Program for Promotion of Fundamental Studies in Health Sciences of the National Institute of Biomedical Innovation, a Grant-in-Aid for Scientific Research from the Ministry of Education, Culture, Sports, Science and Technology of Japan, and a Grant-in-Aid for Scientific Research from the Ministry of Health, Labour and Welfare of Japan.

References

Baba M., Nakajo S., Tu P. H., Tomita T., Nakaya K., Lee V. M., Trojanowski J. Q. and Iwatsubo T. (1998) Aggregation of alpha-synuclein in Lewy bodies of sporadic Parkinson's disease and dementia with Lewy bodies. *Am. J. Pathol.* **152**, 879–884.

Castegna A., Thongboonkerd V., Klein J., Lynn B. C., Wang Y. L., Osaka H., Wada K. and Butterfield D. A. (2004) Proteomic analysis of brain proteins in the gracile axonal dystrophy (gad) mouse, a syndrome that emanates from dysfunctional ubiquitin carboxyl-terminal hydrolase L-1, reveals oxidation of key proteins. *J. Neurochem.* **88**, 1540–1546.

Chandra S., Gallardo G., Fernandez-Chacon R., Schluter O. M. and Sudhof T. C. (2005) Alpha-synuclein cooperates with CSPalpha in preventing neurodegeneration. *Cell* **123**, 383–396.

Choi J., Levey A. I., Weintraub S. T., Rees H. D., Gearing M., Chin L. S. and Li L. (2004) Oxidative modifications and down-regulation of ubiquitin carboxyl-terminal hydrolase L1 associated with idiopathic Parkinson's and Alzheimer's diseases. *J. Biol. Chem.* **279**, 13256–13264.

Chu Y. and Kordower J. H. (2007) Age-associated increases of alpha-synuclein in monkeys and humans are associated with nigrostriatal dopamine depletion: is this the target for Parkinson's disease? *Neurobiol. Dis.* **25**, 134–149.

Conway K. A., Rochet J. C., Bieganski R. M. and Lansbury P. T. Jr (2001) Kinetic stabilization of the alpha-synuclein protofibril by a dopamine-alpha-synuclein adduct. *Science* **294**, 1346–1349.

da Costa C. A., Ancolio K. and Checler F. (2000) Wild-type but not Parkinson's disease-related ala-53 –> Thr mutant alpha-synuclein protects neuronal cells from apoptotic stimuli. *J. Biol. Chem.* **275**, 24065–24069.

Farrer M. J. (2006) Genetics of Parkinson disease: paradigm shifts and future prospects. *Nat. Rev. Genet.* **7**, 306–318.

Furuya T., Hayakawa H., Yamada M., Yoshimi K., Hisahara S., Miura M., Mizuno Y. and Mochizuki H. (2004) Caspase-11 mediates inflammatory dopaminergic cell death in the 1-methyl-4-phenyl-1,2,3,6-tetrahydropyridine mouse model of Parkinson's disease. *J. Neurosci.* **24**, 1865–1872.

Gong B., Cao Z., Zheng P., Vitolo O. V., Liu S., Staniszewski A., Moolman D., Zhang H., Shelanski M. and Arancio O. (2006) Ubiquitin hydrolase Uch-L1 rescues beta-amyloid-induced decreases in synaptic function and contextual memory. *Cell* **126**, 775–788.

Gorbatyuk O. S., Li S., Sullivan L. F., Chen W., Kondrikova G., Manfredsson F. P., Mandel R. J. and Muzyczka N. (2008) The

phosphorylation state of Ser-129 in human alpha-synuclein determines neurodegeneration in a rat model of Parkinson disease. *Proc. Natl Acad. Sci. USA* **105**, 763–768.

Harada T., Harada C., Wang Y. L. *et al.* (2004) Role of ubiquitin carboxy terminal hydrolase-L1 in neural cell apoptosis induced by ischemic retinal injury in vivo. *Am. J. Pathol.* **164**, 59–64.

Kabuta T. and Wada K. (2008) Insights into links between familial and sporadic Parkinson's disease: physical relationship between UCH-L1 variants and chaperone-mediated autophagy. *Autophagy* **4**, 827–829.

Kabuta T., Furuta A., Aoki S., Furuta K. and Wada K. (2008a) Aberrant interaction between Parkinson's disease-associated mutant UCH-L1 and the lysosomal receptor for chaperone-mediated autophagy. *J. Biol. Chem.* **283**, 23731–23738.

Kabuta T., Setsuie R., Mitsui T., Kinugawa A., Sakurai M., Aoki S., Uchida K. and Wada K. (2008b) Aberrant molecular properties shared by familial Parkinson's disease-associated mutant UCH-L1 and carbonyl-modified UCH-L1. *Hum. Mol. Genet.* **17**, 1482–1496.

Kirik D., Rosenblad C., Burger C., Lundberg C., Johansen T. E., Muzyczka N., Mandel R. J. and Bjorklund A. (2002) Parkinson-like neurodegeneration induced by targeted overexpression of alpha-synuclein in the nigrostriatal system. *J. Neurosci.* **22**, 2780–2791.

Kirik D., Annett L. E., Burger C., Muzyczka N., Mandel R. J. and Bjorklund A. (2003) Nigrostriatal alpha-synucleinopathy induced by viral vector-mediated overexpression of human alpha-synuclein: a new primate model of Parkinson's disease. *Proc. Natl Acad. Sci. USA* **100**, 2884–2889.

Kruger R., Kuhn W., Muller T., Woitalla D., Graeber M., Kosel S., Przuntek H., Epplen J. T., Schols L. and Riess O. (1998) Ala30Pro mutation in the gene encoding alpha-synuclein in Parkinson's disease. *Nat. Genet.* **18**, 106–108.

Kurihara L. J., Kikuchi T., Wada K. and Tilghman S. M. (2001) Loss of Uch-L1 and Uch-L3 leads to neurodegeneration, posterior paralysis and dysphagia. *Hum. Mol. Genet.* **10**, 1963–1970.

Larsen C. N., Price J. S. and Wilkinson K. D. (1996) Substrate binding and catalysis by ubiquitin C-terminal hydrolases: identification of two active site residues. *Biochemistry* **35**, 6735–6744.

Larsen C. N., Krantz B. A. and Wilkinson K. D. (1998) Substrate specificity of deubiquitinating enzymes: ubiquitin C-terminal hydrolases. *Biochemistry* **37**, 3358–3368.

Leroy E., Boyer R., Auburger G. *et al.* (1998) The ubiquitin pathway in Parkinson's disease. *Nature* **395**, 451–452.

Li W., Lesuisse C., Xu Y., Troncoso J. C., Price D. L. and Lee M. K. (2004) Stabilization of alpha-synuclein protein with aging and familial Parkinson's disease-linked A53T mutation. *J. Neurosci.* **24**, 7400–7409.

Liu Y., Fallon L., Lashuel H. A., Liu Z. and Lansbury P. T. Jr (2002) The UCH-L1 gene encodes two opposing enzymatic activities that affect alpha-synuclein degradation and Parkinson's disease susceptibility. *Cell* **111**, 209–218.

Lo Bianco C., Ridet J. L., Schneider B. L., Deglon N. and Aebischer P. (2002) Alpha-synucleinopathy and selective dopaminergic neuron loss in a rat lentiviral-based model of Parkinson's disease. *Proc. Natl Acad. Sci. USA* **99**, 10813–10818.

Lombardino A. J., Li X. C., Hertel M. and Nottebohm F. (2005) Replaceable neurons and neurodegenerative disease share depressed UCHL1 levels. *Proc. Natl Acad. Sci. USA* **102**, 8036–8041.

Lowe J., McDermott H., Landon M., Mayer R. J. and Wilkinson K. D. (1990) Ubiquitin carboxyl-terminal hydrolase (PGP 9.5) is selectively present in ubiquitinated inclusion bodies characteristic of human neurodegenerative diseases. *J. Pathol.* **161**, 153–160.

Mandir A. S., Przedborski S., Jackson-Lewis V., Wang Z. Q., Simbulan-Rosental C. M., Smulson M. E., Hoffman B. E., Guastella D. B., Dawson V. L. and Dawson T. M. (1999) Poly(ADP-ribose) polymerase activation mediates 1-methyl-4-phenyl-1,2,3,6-tetrahydropyridine (MPTP)-induced parkinsonism. *Proc. Natl Acad. Sci. USA* **96**, 5774–5779.

Miura H., Oda K., Endo C., Yamazaki K., Shibasaki H. and Kikuchi T. (1993) Progressive degeneration of motor nerve terminals in GAD mutant mouse with hereditary sensory axonopathy. *Neuropathol. Appl. Neurobiol.* **19**, 41–51.

Mosharov E. V., Staal R. G., Bove J. *et al.* (2006) Alpha-synuclein overexpression increases cytosolic catecholamine concentration. *J. Neurosci.* **26**, 9304–9311.

Nishikawa K., Li H., Kawamura R. *et al.* (2003) Alterations of structure and hydrolase activity of parkinsonism-associated human ubiquitin carboxyl-terminal hydrolase L1 variants. *Biochem. Biophys. Res. Commun.* **304**, 176–183.

Nishioka K., Hayashi S., Farrer M. J. *et al.* (2006) Clinical heterogeneity of alpha-synuclein gene duplication in Parkinson's disease. *Ann. Neurol.* **59**, 298–309.

Norris E. H., Giasson B. I., Hodara R., Xu S., Trojanowski J. Q., Ischiropoulos H. and Lee V. M. (2005) Reversible inhibition of alpha-synuclein fibrillization by dopaminochrome-mediated conformational alterations. *J. Biol. Chem.* **280**, 21212–21219.

Oda K., Yamazaki K., Miura H., Shibasaki H. and Kikuchi T. (1992) Dying back type axonal degeneration of sensory nerve terminals in muscle spindles of the gracile axonal dystrophy (GAD) mutant mouse. *Neuropathol. Appl. Neurobiol.* **18**, 265–281.

Osaka H., Wang Y. L., Takada K. *et al.* (2003) Ubiquitin carboxy-terminal hydrolase L1 binds to and stabilizes monoubiquitin in neuron. *Hum. Mol. Genet.* **12**, 1945–1958.

Polymeropoulos M. H., Lavedan C., Leroy E. *et al.* (1997) Mutation in the alpha-synuclein gene identified in families with Parkinson's disease. *Science* **276**, 2045–2047.

Ramirez A., Heimbach A., Grundemann J. *et al.* (2006) Hereditary parkinsonism with dementia is caused by mutations in ATP13A2, encoding a lysosomal type 5 P-type ATPase. *Nat. Genet.* **38**, 1184–1191.

Saigoh K., Wang Y. L., Suh J. G. *et al.* (1999) Intragenic deletion in the gene encoding ubiquitin carboxy-terminal hydrolase in gad mice. *Nat. Genet.* **23**, 47–51.

Sambrook J. and Russell D. W. (2001) *Molecular Cloning: A Laboratory Manual*, 3rd edn. Cold Spring Harbor Laboratory Press, Cold Spring Harbor, NY.

Setsuie R., Wang Y. L., Mochizuki H. *et al.* (2007) Dopaminergic neuronal loss in transgenic mice expressing the Parkinson's disease-associated UCH-L1 I93M mutant. *Neurochem. Int.* **50**, 119–129.

Singleton A. B., Farrer M., Johnson J. *et al.* (2003) Alpha-synuclein locus triplication causes Parkinson's disease. *Science* **302**, 841.

Spillantini M. G., Schmidt M. L., Lee V. M., Trojanowski J. Q., Jakes R. and Goedert M. (1997) Alpha-synuclein in Lewy bodies. *Nature* **388**, 839–840.

Wilkinson K. D., Lee K. M., Deshpande S., Duerksen-Hughes P., Boss J. M. and Pohl J. (1989) The neuron-specific protein PGP 9.5 is a ubiquitin carboxyl-terminal hydrolase. *Science* **246**, 670–673.

Xu J., Kao S. Y., Lee F. J., Song W., Jin L. W. and Yankner B. A. (2002) Dopamine-dependent neurotoxicity of alpha-synuclein: a mechanism for selective neurodegeneration in Parkinson disease. *Nat. Med.* **8**, 600–606.

Yamada M., Iwatsubo T., Mizuno Y. and Mochizuki H. (2004) Overexpression of alpha-synuclein in rat substantia nigra results in loss of dopaminergic neurons, phosphorylation of alpha-synuclein and activation of caspase-9: resemblance to pathogenetic changes in Parkinson's disease. *J. Neurochem.* **91**, 451–461.

Yasuda T., Miyachi S., Kitagawa R. *et al.* (2007) Neuronal specificity of alpha-synuclein toxicity and effect of Parkin co-expression in primates. *Neuroscience* **144**, 743–753.

Zarranz J. J., Alegre J., Gomez-Esteban J. C. *et al.* (2004) The new mutation, E46K, of alpha-synuclein causes Parkinson and Lewy body dementia. *Ann. Neurol.* **55**, 164–173.

Zhou Y., Gu G., Goodlett D. R., Zhang T., Pan C., Montine T. J., Montine K. S., Aebersold R. H. and Zhang J. (2004) Analysis of alpha-synuclein-associated proteins by quantitative proteomics. *J. Biol. Chem.* **279**, 39155–39164.

Neurochemistry International xxx (2009) xxx–xxx

Contents lists available at ScienceDirect

Neurochemistry International

journal homepage: www.elsevier.com/locate/neuint

Proteomic and histochemical analysis of proteins involved in the dying-back-type of axonal degeneration in the gracile axonal dystrophy (*gad*) mouse

Akiko Goto [a,b], Yu-Lai Wang [a], Tomohiro Kabuta [a], Rieko Setsuie [a], Hitoshi Osaka [a], Akira Sawa [c], Shoichi Ishiura [b], Keiji Wada [a,*]

[a] Department of Degenerative Neurological Diseases, National Institute of Neuroscience, National Center of Neurology and Psychiatry, 4-1-1 Ogawahigashi, Kodaira, Tokyo, 187-8502, Japan
[b] Department of Life Sciences, Graduate School of Arts and Sciences, University of Tokyo, 3-8-1 Komaba, Meguro-ku, Tokyo,153-8902, Japan
[c] Depts. of Psychiatry and Neuroscience, Johns Hopkins University School of Medicine, Baltimore, MD 21287, USA

ARTICLE INFO

Article history:
Received 24 November 2008
Received in revised form 12 December 2008
Accepted 17 December 2008

Keywords:
Axonal degeneration
Dying-back
gad mouse
UCH-L1
Ubiquitin
2D-DiGE
GAPDH
Oxidative stress

ABSTRACT

Local axonal degeneration is a common pathological feature of peripheral neuropathies and neurodegenerative disorders of the central nervous system, including Alzheimer's disease, Parkinson's disease, and stroke; however, the underlying molecular mechanism is not known. Here, we analyzed the gracile axonal dystrophy (*gad*) mouse, which displays the dying-back-type of axonal degeneration in sensory neurons, to find the molecules involved in the mechanism of axonal degeneration. The *gad* mouse is analogous to a null mutant of ubiquitin carboxyl-terminal hydrolase L1 (UCH-L1). UCH-L1 is a deubiquitinating enzyme expressed at high levels in neurons, as well as testis and ovary. In addition, we recently discovered a new function of UCH-L1—namely to bind to and stabilize mono-ubiquitin in neurons, and found that the level of mono-ubiquitin was decreased in neurons, especially in axons of the sciatic nerve, in *gad* mice. The low level of ubiquitin suggests that the target proteins of the ubiquitin proteasome system are not sufficiently ubiquitinated and thus degraded in the *gad* mouse; therefore, these proteins may be the key molecules involved in axonal degeneration. To identify molecules involved in axonal degeneration in *gad* mice, we compared protein expression in sciatic nerves between *gad* and wild-type mice at 2 and 12 weeks old, using two-dimensional difference gel electrophoresis. As a result, we found age-dependent accumulation of several proteins, including glyceraldehyde-3-phosphate dehydrogenase (GAPDH) and 14-3-3, in *gad* mice compared with wild-type mice. Histochemical analyses demonstrated that GAPDH and 14-3-3 were localized throughout axons in both *gad* and wild-type mice, but GAPDH accumulated in the axons of *gad* mice. Recently, it has been suggested that a wide range of neurodegenerative diseases are characterized by the accumulation of intracellular and extracellular protein aggregates, and it has been reported that oxidative stress causes the aggregation of GAPDH. Furthermore, histochemical analysis demonstrated that sulfonated GAPDH, a sensor of oxidative stress that elicits cellular dysfunction, was expressed in the axons of *gad* mice, and 4-hydroxy-2-nonenal, a major marker of oxidative stress, was also only detected in *gad* mice. Our findings suggest that GAPDH may participate in a process of the dying-back-type of axonal degeneration in *gad* mice and may provide valuable insight into the mechanisms of axonal degeneration.

1. Introduction

Axonal degeneration occurs in several chronic neurodegenerative diseases and in injuries caused by, for example, toxic, ischemic, or traumatic insults. Recent findings suggest that axonal degeneration precedes, and sometimes causes, neuronal death in these neurodegenerative disorders (Li et al., 2001; Ferri et al., 2003; Fischer et al., 2004; Stokin et al., 2005; Fischer and Glass, 2007), but the underlying molecular mechanism is not known.

The gracile axonal dystrophy (*gad*) mutant mouse is characterized by sensory ataxia at an early stage, followed by motor ataxia at a later stage (Yamazaki et al., 1988; Saigoh et al., 1999). Pathologically, axonal degeneration in the *gad* mouse begins with the distal ends of primary ascending axons in the dorsal root ganglia (DRG) (Mukoyama et al., 1989; Kikuchi et al., 1990; Oda et al., 1992; Miura et al., 1993), and spheroid formation in the dying-back-type of axonal degeneration is observed in the gracile and dorsal spinocerebellar tracts (Yamazaki et al., 1988; Kikuchi

* Corresponding author. Tel.: +81 42 346 1715 fax: +81 42 346 1745.
E-mail address: wada@ncnp.go.jp (K. Wada).

0197-0186/$ – see front matter © 2008 Elsevier Ltd. All rights reserved.
doi:10.1016/j.neuint.2008.12.012

Please cite this article in press as: Goto, A., et al., Proteomic and histochemical analysis of proteins involved in the dying-back-type of axonal degeneration in the gracile axonal dystrophy (*gad*) mouse. Neurochem. Int. (2009), doi:10.1016/j.neuint.2008.12.012

et al., 1990; Miura et al., 1993). At a later stage, axonal degeneration and spheroid formation are observed at both the central and peripheral ends of DRG neurons and extend transsynaptically to the upper tracts as well as to motor neurons (Mukoyama et al., 1989; Kikuchi et al., 1990; Oda et al., 1992; Miura et al., 1993). Therefore, the *gad* mouse is an effective model for analyzing the molecular mechanism of the dying-back-type of axonal degeneration.

Previously, we found that the *gad* mutation is caused by an in-frame deletion of *Uchl1*, which encodes ubiquitin carboxyl-terminal hydrolase L1 (UCH-L1) (Saigoh et al., 1999). UCH-L1 is expressed at high levels in neurons, as well as testis and ovary, and constitutes ~5% of total soluble protein in the brain (Wilkinson et al., 1989). UCH-L1 is reported to be one of the deubiquitinating enzymes in the ubiquitin-proteasome system (UPS), where it hydrolyzes bonds between ubiquitin (Ub) and small adducts and creates free mono-Ub *in vitro* (Larsen et al., 1998). UCH-L1 also acts as a Ub ligase *in vitro* (Liu et al., 2002). In addition, we recently found a new function for UCH-L1—to bind to and stabilize mono-Ub in neurons (Osaka et al., 2003).

Using histochemical analysis, we previously demonstrated that UCH-L1 and mono-Ub are colocalized in axons of the sciatic nerve. In *gad* mice, the level of mono-Ub was decreased in neurons, especially in axons of the sciatic nerve (Osaka et al., 2003). The low level of ubiquitin suggests that the target proteins of the ubiquitin-proteasome system (UPS) are not sufficiently ubiquitinated and thus degraded in the *gad* mouse; therefore, these proteins may be key molecules involved in axonal degeneration. To identify the molecules involved in axonal degeneration in *gad* mice, we analyzed protein expression in sciatic nerves using two-dimensional difference gel electrophoresis (2D-DIGE).

Proteomic approaches compare protein expression comprehensively; 2D-DIGE is a modification of the traditional 2D technology, in which small amounts of multiple protein samples can be compared together, because each sample can be pre-labeled with different fluorescence dyes, mixed together, and run on the same isoelectric focusing (IEF) gel and SDS-PAGE (Knowles et al., 2003; Shaw and Riederer, 2003). We used 2D-DIGE because it is the most efficient method for analyzing the small amount of protein that can be extracted from a sciatic nerve. Here, we show that there are age-dependent accumulations of several proteins, including glyceraldehyde-3-phosphate dehydrogenase (GAPDH) and 14-3-3, in *gad* mice compared with wild-type (WT) mice, suggesting that these proteins are involved in axonal degeneration.

2. Experimental procedures

2.1. Animals

We used homozygous *gad* mice and their wild-type siblings (Harada et al., 2004; Wang et al., 2004). Mice were maintained and propagated at the National Institute of Neuroscience, National Center of Neurology and Psychiatry, Japan. Proteomic studies were carried out at 2 and 12 weeks old. Western blotting analyses were carried out at 12 weeks old. Histochemical analyses were carried out at 7 and 12 weeks old. Animals were anesthetized with Nembutal, and the sciatic nerve was perfused with saline. All mouse experiments were performed in accordance with our institution's regulations for animal care and with the approval of the Animal Investigation Committee of the National Institute of Neuroscience, National Center of Neurology and Psychiatry which conforms to the National Institute of Health guide for the care and use of laboratory animals.

2.2. Preparation of protein samples and labeling of protein samples with Cy dyes

Each sciatic nerve was suspended in 300 μl of sample buffer, containing 7 M urea, 2 M thiourea, 4% (w/v) CHAPS, and 40 mM Tris base (pH 8.0), by sonication for 60 s on ice, gently vortexed, and centrifuged for 20 min at 14,000 × *g* at 4 °C. Protein concentration was determined using a 2-D Quant Kit (GE Healthcare, Piscataway, NJ, USA). Protein samples were labeled as recommended by the manufacturer (GE Healthcare) using 400 pmol Cy dyes (GE Healthcare) per 50 μg of protein. Separate solutions containing 15 μg of protein from one *gad* or WT sample were labeled with Cy3 or Cy5 dye, respectively, and a common pool of proteins with *gad* and WT samples mixed equally were labeled with Cy2 dye by vortexing and incubating on ice in the dark for 30 min. The labeled samples were quenched by the addition of 1 μl 10 mM lysine (Sigma–Aldrich, St. Louis, MO, USA) and incubated on ice for 10 min.

2.3. Two-dimensional polyacrylamide gel electrophoresis (2D PAGE)

The quenched Cy3, Cy5, and Cy2 samples (15 μg of protein each) were mixed and denatured in 2D PAGE sample buffer containing 7 M urea, 2 M thiourea, 4% (w/v) CHAPS, 0.2% DTT, and 1.4% Ampholine. For the IEF, 45 μg of protein was applied to a rehydrated Immobiline Drystrip (pH 3–10, 7 cm; GE Healthcare) in a strip holder and incubated overnight in the dark. IEF was performed using a Multiphor II Electrophoresis system (GE Healthcare). The electrophoresis conditions were set as follows: step 1, 200 V for 1 min; step 2, 3500 V for 90 min; step 3, 3500 V for 125 min. After IEF, the strip was equilibrated with SDS buffer and applied to the 12.5% 2D SDS-PAGE for the analysis of 12-week-old mice and to the 4–20% SDS-PAGE for the analysis of 2-week-old mice using a precast Multigel II system (Daiichi Kagaku, Japan).

2.4. Image analysis and statistics

We scanned 2D gels using a Typhoon 9000 fluorescent imager (GE Healthcare). Excitation/emission wavelengths were chosen for each of the dyes. Gel images were preprocessed to remove extraneous areas using ImageQuant V5.0 (GE Healthcare). Gel analysis was performed using DeCyder DIA V5.0 (Difference In-gel Analysis; GE Healthcare). In-gel matching and statistical analysis were performed using DeCyder BVA V5.0 (Biological Variance Analysis; GE Healthcare). The Student's paired *t*-test ($P < 0.05$) was performed to identify the protein spots that were differentially expressed between *gad* and WT mice.

2.5. In-gel digestion and analysis by matrix-assisted laser desorption/ionization tandem time-of-flight (MALDI-TOF/TOF) mass spectrometry

To identify a particular protein in a spot detected by 2D-DIGE analysis, sciatic nerve extract containing 100 μg of protein was subjected to 12.5% 2D SDS-PAGE and stained with Coomassie brilliant blue (Invitrogen). The spots of interest were excised from the gel, destained, dehydrated with acetonitrile for 10 min, and completely dried under a vacuum pump for 10 min. Each spot was placed in 20 μl of 5 mM NH_4HCO_3 containing 1 pmol of sequencing-grade trypsin (Promega, Madison, WI, USA) overnight at 37 °C. Aliquots of the trypsinized samples were analyzed by nanoliquid chromatography and automatically spotted with alpha-cyano-4-hydroxy-cinnamic acid solution on a stainless-steel target and air dried. All mass spectra were obtained with MALDI-TOF/TOF (AXIMA-CFR; Shimadzu, Japan). MALDI peptide spectra were calibrated using several peaks of self-digested trypsin and matrix ion as internal standards.

2.6. Protein identification

Protein identification was performed using database searches on the web with Mascot Wizard (Matrix Science Ltd., London, United Kingdom). Criteria for protein identification were as follows: mascot score higher than 80 and mass tolerance of 100 ppm. Calculated pI and molecular mass data were obtained by Mascot.

2.7. 2D Western blotting for identification of GAPDH

One protein spot that was increased in *gad* mice but could not be detected by MALDI-TOF/TOF analysis was speculated to be GAPDH from its isoelectric point, molecular weight and location of the 2D gel compared with the mouse brain proteome database, and was therefore subjected to 2D Western blotting using an anti-GAPDH antibody (1:200, Chemicon, MAB374). One-hundred μg of sciatic nerve proteins were separated by 12.5% 2D SDS-PAGE and transferred onto a PVDF membrane (Immobilon-P; Millipore, Bedford, MA, USA). The membrane was washed with MilliQ water for 1 h at room temperature. Western blotting was performed as described in the following section.

2.8. Western blotting

Using 4–20% gradient SDS-PAGE, 2 μg of total protein was separated and transferred onto a PVDF membrane (Immobilon-P; Millipore). The membrane was washed with MilliQ water, then blocked with 5% skim milk in 0.05% Tween 20 in TBS (TTBS) for 1 h at room temperature, and incubated with primary antibodies in TTBS overnight at 4 °C. Primary antibodies used in this study were anti-UCH-L1 polyclonal antibody (1:5000, UltraClone, RA95101), anti-GAPDH monoclonal antibody (1:200, Chemicon, MAB374), anti-14-3-3 polyclonal antibody (1:100, IBL, 18649), anti-neurofilament L monoclonal antibody (NF-L, 1:500, Chemicon, MAB1615), anti-neuronal class III β tubulin antibody (βTUBIII, 1:1000, Covance, TUJ1), and anti-actin monoclonal antibody (1:4000, Sigma, AC-15). After washing, the membranes were incubated for 1 h at room temperature with either anti-mouse or anti-rabbit IgG horseradish peroxidase (HRP) conjugated secondary antibodies (1:10,000, GE Healthcare). Protein signals were detected with SuperSignal West Femto Maximum Sensitivity Substrate (Pierce) and were visualized with the LAS-3000 imaging system (Fujifilm, Tokyo, Japan).

Please cite this article in press as: Goto, A., et al., Proteomic and histochemical analysis of proteins involved in the dying-back-type of axonal degeneration in the gracile axonal dystrophy (*gad*) mouse. Neurochem. Int. (2009), doi:10.1016/j.neuint.2008.12.012

2.9. Immunohistochemistry

Mice were anesthetized and perfused with ice-cold 4% paraformaldehyde in phosphate-buffered saline (PBS, pH 7.4). Sciatic nerves were collected and postfixed in 4% paraformaldehyde overnight at 4 °C. The samples were embedded in paraffin and sectioned at 5 μm for immunohistochemistry. Serial sections were deparaffinized in xylene and graded ethanol, and washed in distilled water. Sections were blocked by incubation in 10% normal goat serum for 30 min at room temperature and incubated overnight at 4 °C with diluted primary antibodies. The following antibodies were used at the final dilutions indicated: anti-GAPDH polyclonal antibody (1:1000), anti-sulfonated GAPDH polyclonal antibody (1:500; these two antibodies were kindly provided by Dr. Sawa), anti-14-3-3 polyclonal antibody (1:100, IBL, 18649), anti-myelin basic protein monoclonal antibody (MBP, 1:200, QED Bioscience, 24201), anti-neurofilament M monoclonal antibody (NF-M, 1:200, Chemicon, MAB1621), anti-UCH-L1 polyclonal antibody (1:2000, UltraClone, RA95101), anti-UCH-L1 monoclonal antibody (1:200; Medac, Wedel, Germany), βTUBIII (1:300, COVANCE, TUJ1), and anti-4-hydroxy-2-nonenal monoclonal antibody (HNE, 25 μg/ml, JaICA, Shizuoka, Japan).

After incubating with primary antibodies, sections were washed 5 times with 0.1% Tween 20 in PBS (PBST) for 5 min at room temperature and then incubated for 90 min at room temperature with diluted secondary antibodies. The following antibodies were used at the final dilutions indicated: anti-mouse-Alexa594 IgG and anti-rabbit-Alexa588 IgG (1:400, Invitrogen) for immunofluorescence staining, or EnVision+ anti-rabbit HRP (Dako, Japan) for DAB staining. For DAB staining, bound antibody complexes were visualized using DAB (Dako, Japan) as a peroxidase substrate. Primary and secondary antibodies were diluted in Dako Antibody Diluent (Dako, Japan). After incubation with secondary antibodies, sections were washed 5 times with PBST for 5 min at room temperature and mounted with Antifade Kit (Molecular Probes). For analysis of 14-3-3 and HNE, sections were pretreated in a microwave oven for 10 min in citrate buffer solution (pH 6.0), cooled down, and washed 3 times for 5 min in PBS at room temperature. For the other immunostaining analyses, this pretreatment was not needed. For DAB staining, sections were treated with 3% H_2O_2 in methanol for 5 min to quench endogenous peroxidase activity before treatment with the primary antibodies.

3. Results

3.1. Analyses of differentially expressed proteins between gad and WT mice by 2D-DIGE

To find proteins that are upregulated in *gad* mice compared with WT mice, we analyzed sciatic nerves from 3 *gad* and 3 WT mice at 2 weeks old as well as at 12 weeks old, using 2D-DIGE technology. The proteins from *gad* mice were pre-labeled with Cy5 (red), and the proteins from WT mice were pre-labeled with Cy3 (green), respectively. A common pool of proteins composed of an equal amount of protein from a single *gad* and WT mouse was pre-labeled with Cy2, and the same manipulation was performed in 3 independent experiments.

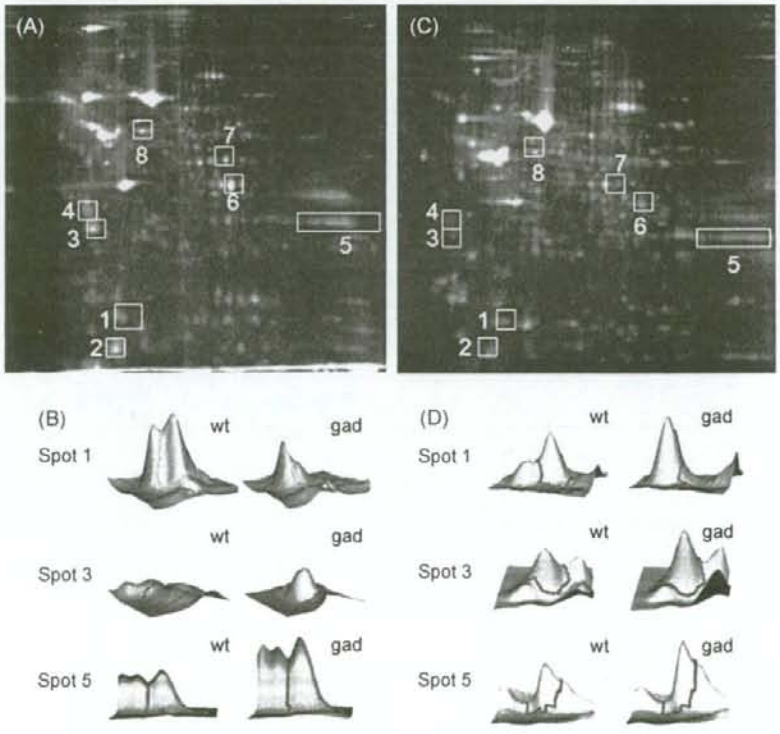

Fig. 1. Analyses of differentially expressed proteins between *gad* and wild-type mice by two-dimensional difference gel electrophoresis (2D-DIGE).
(A) A representative pseudocolor picture of superimposed DIGE images of mice at 12 weeks old. Fourteen protein spots are increased in *gad* mice compared with wild-type (WT) mice (red) by at least 1.6-fold (Student's paired *t*-test value; $P < 0.05$ in 3 parallel gels), and one spot is not detected at all in *gad* mice (green). Seven protein spots (spot No. 2–8) are increased in *gad* mice in an age-dependent manner, and one spot (spot No. 1) was not detected at all in *gad* mice at either 2 or 12 weeks old. The spot numbers of the latter differentiated 8 spots are shown in this map.
(B) A representative pseudocolor picture of superimposed DIGE images of mice at 2 weeks old. Eighteen protein spots are increased in *gad* mice compared with WT mice (red) by at least 1.6-fold (Student's paired *t*-test value; $P < 0.05$ in 3 parallel gels), and one spot is not detected at all in *gad* mice (green). The spot numbers in this figure are the same as in A.
(C) The 3D images of typical protein spots that were differentially expressed between *gad* and WT mice at 2 weeks old (spot numbers 1, 3, and 5 in A).
(D) The 3D images of typical protein spots that were differentially expressed between *gad* and WT mice at 2 weeks old (spot numbers 1, 3, and 5 in C) (For interpretation of the references to color in this figure legend, the reader is referred to the web version of the article.)

Please cite this article in press as: Goto, A., et al., Proteomic and histochemical analysis of proteins involved in the dying-back-type of axonal degeneration in the gracile axonal dystrophy (*gad*) mouse. Neurochem. Int. (2009), doi:10.1016/j.neuint.2008.12.012

Table 1
List of proteins differentially expressed between *gad* and WT mice.

Spot no.	Protein name	Score	Molecular mass (kDa)/pI	Av. ratio (*gad*/wt) 12 weeks	*P* value	Av. ratio (*gad*/wt) 2 weeks	*P* value
1	Ubiquitin thiolesterase PGP9.5 (UCH-L1)	96	25.10/5.12	−14.38	0.005	−3.89	0.003
3	14-3-3 protein	94	28.10/4.63	5.4	0.030	7.32	0.001
4	Annexin A5	143	35.79/4.83	6.68	0.020	5.19	0.030
8	Neurofilament triplet L protein (NF-L)	212	61.40/4.62	2.18	0.010	3.53	0.026
5	Glyceraldehyde 3-phosphate dehydrogenase (GAPDH)		38.07/8.34	3.89	0.043	1.61	

*GAPDH was detected by 2D Western blotting and not by MALDI-TOF/TOF.

Fig. 1A shows a representative pseudocolor picture of superimposed DIGE images of the 12-week-old mouse samples. Fourteen protein spots were increased by at least 1.6-fold in *gad* mice compared with WT mice (red; Student's paired *t*-test value; $P < 0.05$ in 3 parallel gels), and one spot was not detected at all in *gad* mice (green).

Fig. 1B shows a representative pseudocolor picture of superimposed DIGE images of the 2-week-old mouse samples. Eighteen protein spots were increased by at least 1.6-fold in *gad* mice compared with WT mice (red; Student's paired *t*-test value; $P < 0.05$ in 3 parallel gels), and one spot was not detected at all in *gad* mice (green).

Based on comparison of the 2D-DIGE analysis of mice between 2 and 12 weeks old, 7 protein spots showed an age-dependent increase in *gad* mice (spots No. 2–8). One spot (spot No. 1) was not detected at all in *gad* mice at either 2 or 12 weeks old (Fig. 1A and B).

Fig. 1C shows the 3D images of typical spots (spots No. 1, 3, and 5) in Fig. 1A, and Fig. 1D shows the 3D images of typical spots (spots No. 1, 3, and 5) in Fig. 1B.

3.2. Identification of differentially expressed proteins between *gad* and WT mice by MALDI-TOF/TOF and 2D Western blotting

The proteins of spots that were age dependently increased or absent in *gad* mice were analyzed by MALDI-TOF/TOF and identified (spots No. 1, 3, 4, and 8). The proteins were identified as UCH-L1 (spot No. 1), 14-3-3 (spot No. 3), annexin V (spot No. 4), and Neurofilament L (NF-L) (spot No. 8). Additionally, we speculated that spot No. 5 may represent GAPDH based on the information from the mouse brain proteome database (http://www.charite.de/humangenetik/klose_public1/index.html), and confirmed this by 2D Western blotting with GAPDH antibodies. The results of the protein identification are listed in Table 1, including spot number, protein name, mascot score, theoretical relative molecular mass, isoelectric point, average ratio of *gad*/wt protein level, and *P*-value using DeCyder, at both 2 and 12 weeks old.

3.3. Analyses of the expression levels of proteins in *gad* and WT mice by Western blotting

In 2D-DIGE system, each sample was pre-labeled with different fluorescence dyes, Cy3, Cy5 or Cy2. This labeling-process allows comparison of multiple samples in same 2D-gel, but it is reported that efficiency of each dyes to label proteins was not exactly the same. We assume that 2D-DIGE is reliable method to detect molecules involved in axonal degeneration but Western blot analysis using specific antibodies is more accurate, and in fact, it is usual that identified proteins by TOF-MASS are reconfirmed by Western blotting. Therefore, the expression levels of the proteins in

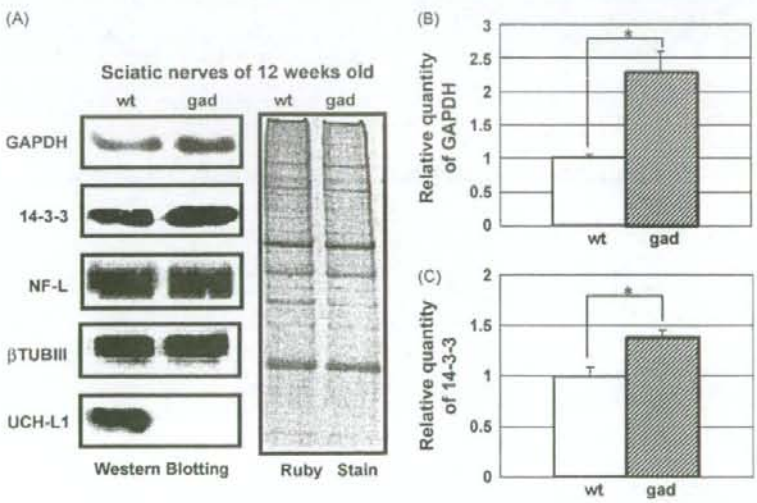

Fig. 2. Western blotting analyses of the expression levels of proteins expressed differentially between *gad* and WT mice.
(A) Results of Western blotting analysis with antibodies against ubiquitin carboxyl-terminal hydrolase L1 (UCH-L1), neurofilament L (NF-L), 14-3-3, glyceraldehyde-3-phosphate dehydrogenase (GAPDH), and classIII β tubulin (βTUBIII). GAPDH and 14-3-3 protein levels were increased in *gad* mice compared with WT mice.
(B) Quantification of the band intensities of GAPDH. Values are means ± SEM of 3 independent experiments (*$P < 0.05$); GAPDH is increased by about 2.3-fold in *gad* mice at 12 weeks old compared with WT mice.
(C) Quantification of the band intensities of 14-3-3. Values are means ± SEM of 3 independent experiments (*$P < 0.05$); 14-3-3 is increased by 1.3-fold in *gad* mice at 12 weeks old compared with WT mice.

Please cite this article in press as: Goto, A., et al., Proteomic and histochemical analysis of proteins involved in the dying-back-type of axonal degeneration in the gracile axonal dystrophy (*gad*) mouse. Neurochem. Int. (2009), doi:10.1016/j.neuint.2008.12.012

gad and WT mice listed in Table 1 were further analyzed by Western blotting to reconfirm the results of 2D-DIGE (Fig. 2A). We chose these proteins because they were all reported to be expressed in neurons. In 12-week-old *gad* mice, GAPDH was increased by an average ratio of 2.3-fold (Fig. 2B), and 14-3-3 was increased by an average ratio of 1.3-fold (Fig. 2C) compared with WT mice. The levels of NF-L and βTUBIII, which was used as an internal control, showed no significant difference between *gad* and WT mice at 12 weeks old (Fig. 2A). Annexin V was not analyzed because its antibodies did not work in this experimental system containing urea and thiourea. The same results were obtained in 3 independent experiments.

3.4. Histochemical localization of GAPDH in the sciatic nerves of gad and WT mice

Sciatic nerves are composed internally of neuronal axons and externally of myelin derived from glial Schwann cells, and protein samples in the proteomic analysis were a mixture of axons and myelin. We examined the histological localization of GAPDH, which was dominantly increased in *gad* mice, by double immunofluorescence staining using an antibody against GAPDH and the neuronal markers neurofilament M (NF-M) or UCH-L1, or the Schwann cells marker myelin basic protein (MBP). In *gad* mice, GAPDH was colocalized with MBP (Fig. 3A, right panel) but was more dominantly colocalized with NF-M, a neuronal marker (Fig. 3A, left panel). These results suggest that GAPDH is mainly localized in axons in *gad* mice. In WT mice, GAPDH was colocalized with the neuronal marker UCH-L1 (Fig. 3B, left panel). Because UCH-L1 is the product of the gene defective in the *gad* mouse, UCH-L1 is not detected in *gad* mice (Fig. 3B, right panel). The same results were obtained in 3 independent experiments.

3.5. DAB staining analyses of GAPDH and 14-3-3 in the sciatic nerves of gad and WT mice

We examined in detail the localization of GAPDH in cross or vertical sections of sciatic nerve axons by DAB staining (Figs. 4A–F). In the cross-sections, GAPDH was localized in axons in both *gad* and WT mice and was remarkably accumulated in *gad* mice compared with WT mice (Fig. 4A and B). In vertical sections, GAPDH was also localized in axons in both *gad* and WT mice (Fig. 4C–F). Notably, aggregates of GAPDH were observed in *gad* mice but not in WT mice (Fig. 4E and F, arrow). Next, we examined the expression of 14-3-3, which was found to be increased in *gad* mice upon 2D-DIGE and Western blotting analyses. In both *gad* and WT mice, 14-3-3 was expressed in axons, and there was no significant difference between *gad* and WT mice (Fig. 4G–J). The same results were obtained in 3 independent experiments.

3.6. Histochemical analyses of sulfonated GAPDH in the sciatic nerves of gad and WT mice

It was reported that oxidative stress induces the oligomerization and aggregation of GAPDH (Cumming and Schubert, 2005; Nakajima et al., 2007), and in this study we found that GAPDH is accumulated in axons of *gad* mice that exhibit a dying-back-type of axonal degeneration. Thus, we postulated that oxidative stress would be increased in *gad* mice, and therefore examined the expression of sulfonated GAPDH (Hara et al., 2005), in the sciatic

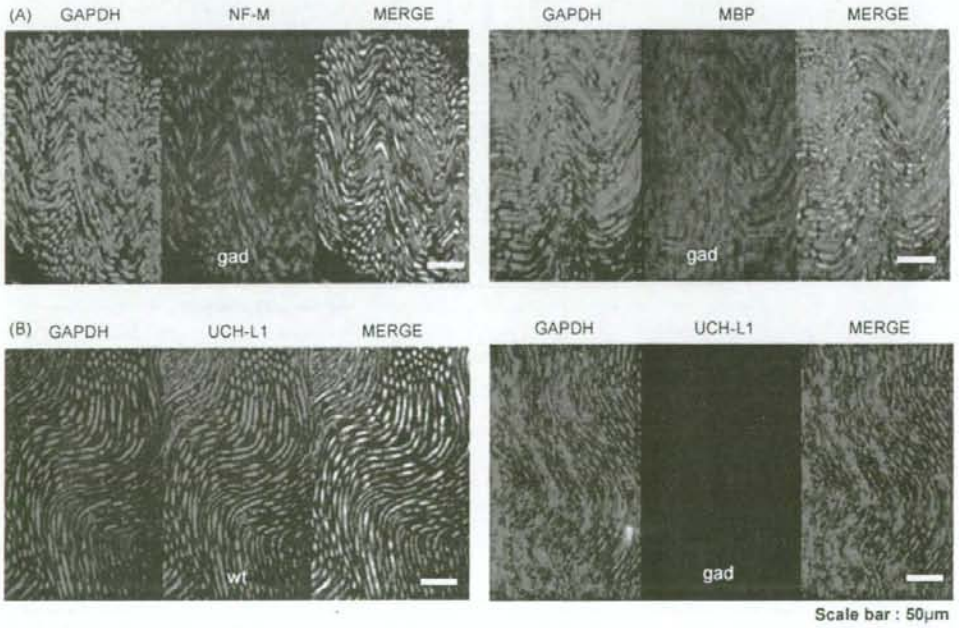

Fig. 3. Histochemical localization of GAPDH in the sciatic nerves of *gad* and WT mice.
(A) Double immunofluorescent staining of the sciatic nerve of *gad* mice using antibodies against GAPDH, neurofilament M (NF-M), or myelin basic protein (MBP). GAPDH was colocalized with NF-M (left panel) and partly with MBP (right panel) in *gad* mice. GAPDH is mainly localized in axons.
(B) Double immunofluorescent staining of the sciatic nerve of *gad* and WT mice using antibodies against GAPDH and UCH-L1. In WT mice, GAPDH is colocalized with UCH-L1 (left panel). In *gad* mice, UCH-L1 is not detected (right panel), and GAPDH is strongly detected compared with WT mice.

Please cite this article in press as: Goto, A., et al., Proteomic and histochemical analysis of proteins involved in the dying-back-type of axonal degeneration in the gracile axonal dystrophy (*gad*) mouse. Neurochem. Int. (2009), doi:10.1016/j.neuint.2008.12.012

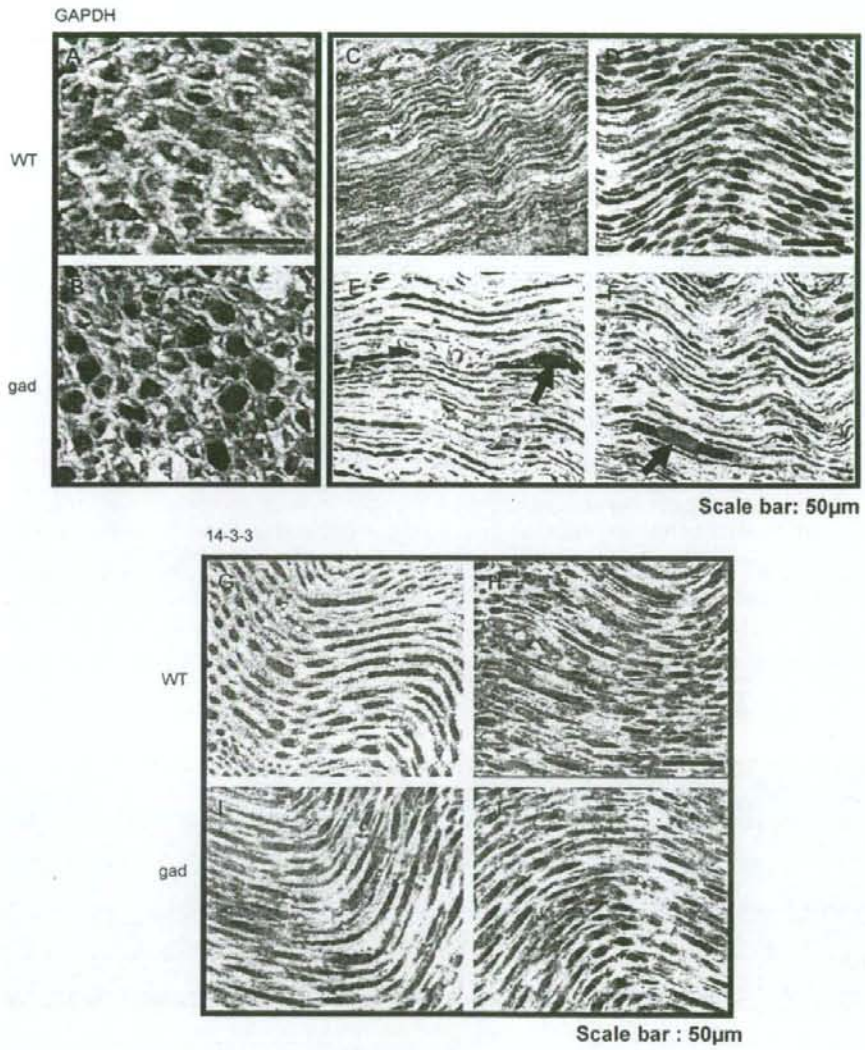

Fig. 4. DAB staining of GAPDH and 14-3-3 in the sciatic nerves of *gad* and WT mice.
(A–F) Sections of sciatic nerves of WT (A, C, and D) or *gad* (B, E, and F) mice stained with DAB using GAPDH antibodies.
(A) Cross-section of a sciatic nerve of a WT mouse. GAPDH is mainly localized in axons.
(B) Cross-section of a sciatic nerve of a *gad* mouse. GAPDH is mainly localized in axons and is highly expressed compared with the WT mouse.
(C and D) Vertical sections of sciatic nerves of WT mice. GAPDH is localized in axons.
(E and F) Vertical sections of sciatic nerves of *gad* mice. GAPDH is localized in axons and is accumulated. GAPDH aggregates are indicated by arrows.
(G–J) Sections of sciatic nerves of WT (G, H) and *gad* (I, J) mice stained with DAB using 14-3-3 antibodies.
(G and H) Vertical sections of sciatic nerves of WT mice; 14-3-3 is localized in axons of WT mice.
(I and J) Vertical sections of sciatic nerves of *gad* mice; 14-3-3 is localized in axons of *gad* mice, and there was no significant difference between *gad* and WT mice (G, H).

nerves of *gad* and WT mice. We found that although sulfonated GAPDH was not detected in WT mice, it was clearly detected in *gad* mice (Fig. 5A and B). In *gad* mice, sulfonated GAPDH was colocalized with the neuronal markers βTUBIII (Fig. 5B) and NF-M (data not shown) in axons. In *gad* mice, accumulated sulfonated GAPDH was also detected in the outer portion of the axons, around the DAPI staining for nuclei (Fig. 5C). Axons do not contain nuclei, so these DAPI signals may come from Schwann cells. The same results were obtained in 3 independent experiments.

3.7. Histological analyses of HNE, a marker of oxidative stress, in the sciatic nerves of gad and WT mice

The results shown in Fig. 5 suggest that the level of oxidative stress is increased in *gad* mice. Accordingly, we examined the existence of HNE, a major marker of oxidative stress, in addition to sulfonated GAPDH. HNE was detected in *gad* mice, but not in WT mice (Fig. 6). The same results were obtained in 3 independent experiments.

Please cite this article in press as: Goto, A., et al., Proteomic and histochemical analysis of proteins involved in the dying-back-type of axonal degeneration in the gracile axonal dystrophy (*gad*) mouse. Neurochem. Int. (2009), doi:10.1016/j.neuint.2008.12.012

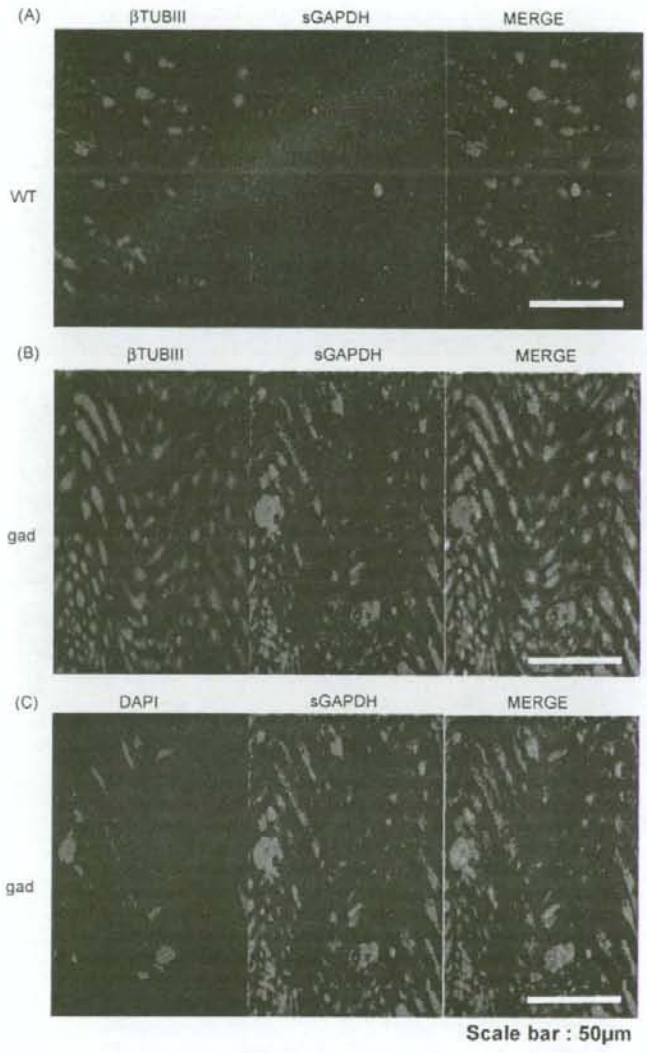

Fig. 5. Expression of sulfonated GAPDH in the sciatic nerves of *gad* and WT mice.
(A) Double immunofluorescent staining of a sciatic nerve of a WT mouse using antibodies against sulfonated GAPDH and βTUBIII. Sulfonated GAPDH was not detected in WT mice (middle panel).
(B) Double immunofluorescent staining of a sciatic nerve of a *gad* mouse using antibodies against sulfonated GAPDH and βTUBIII. In *gad* mice, sulfonated GAPDH was detected in axons of sciatic nerves (middle panel). Sulfonated GAPDH was colocalized with the neuronal marker βTUBIII in *gad* mice (right panel), as well as NF-M (data not shown). A representative result from 3 independent experiments is shown.
(C) Double immunofluorescent staining of a sciatic nerve of the *gad* mouse using an antibody against sulfonated GAPDH and DAPI. Sulfonated GAPDH was detected uniformaly within the axons of *gad* mice, and accumulation of sulfonated GAPDH was detected around the DAPI signals (right panel).

4. Discussion

In this study, we found that 14-3-3, annexin V, NF-L, and GAPDH were increased in an age-dependent manner in *gad* mice that display the dying-back-type of axonal degeneration, using 2D-DIGE analyses (Fig. 1). Based on Western blotting analyses, 14-3-3 and GAPDH were increased in *gad* mice compared with WT mice (Fig. 2). Histochemical analysis revealed that GAPDH was localized throughout axons and was accumulated in axons in *gad* mice compared with WT mice (Figs. 3 and 4). Also 14-3-3 was localized throughout axons, but there was no significant difference between *gad* and WT mice upon histochemical analyses, although it was increased in *gad* mice upon Western blotting analyses (Fig. 4). Since Western blotting showed only a slight increase in 14-3-3 (Fig. 2), we assume that this small difference could not be detected by histochemical analyses.

GAPDH is a classic glycolytic enzyme (Sirover, 1999; Chuang et al., 2005), and recent studies show that it is multifunctional

Please cite this article in press as: Goto, A., et al., Proteomic and histochemical analysis of proteins involved in the dying-back-type of axonal degeneration in the gracile axonal dystrophy (*gad*) mouse. Neurochem. Int. (2009), doi:10.1016/j.neuint.2008.12.012